UNIVERSITAT POLITÈCNICA DE CATALUNYA
BARCELONATECH

MASTER THESIS

Simulation of the gas phase integration between compartments CIVa and CV of the MELiSSA Pilot Plant

Sergio Pilo Teniente

SUPERVISED BY

Francesc Gòdia Casablancas
and Enrique Peiro Cezón

Universitat Politècnica de Catalunya
Master in Aerospace Science & Technology
July 2015

Simulation of the gas phase integration between compartments CIVa and CV of the MELiSSA Pilot Plant

BY

Sergio Pilo Teniente

DIPLOMA THESIS FOR DEGREE

Master in Aerospace Science and Technology

AT

Universitat Politècnica de Catalunya

SUPERVISED BY:

Francesc Gòdia Casablancas
and Enrique Peiro Cezón

MELiSSA Pilot Plant – Claude Chipaux Laboratory
Department of Chemical Engineering
Universitat Autònoma de Barcelona

ABSTRACT

The MELiSSA Pilot Plant, situated at the UAB (Barcelona), is a facility created to demonstrate the MELiSSA project, an international European project developing a closed regenerative system to provide life support in Space. After years of research and development, the first integration step has just started and the others will take place in the coming years.

In this context, this thesis addresses a simulation tool to assess the MELiSSA first integration step and pave the way to the next ones. Therefore, the main objectives of this project can be summarized as follows:

- To define the model used for the first MELiSSA integration step.
- To simulate the integration step and compare the results with data acquired from the real experiment carried out at the MELiSSA Pilot Plant.
- To exploit the simulation tool in order to see how the system would behave in different scenarios with different working conditions and the effect of potential perturbations.

In order to carry out the simulation, MATLAB-SIMULINK software has been used. Starting from a model originally created by Laurent Poughon (Axe Génie des Procédés Energétique et Biosystèmes, Université Blaise Pascal, Clermont-Ferrand, France), it has been adapted to the specific needs of the MELiSSA first integration step.

The results obtained have shown that, despite the complexity of the real experiment involving two very distinct biological systems, the model gets closer to reality in many respects. Even so, more research regarding specific issues is needed to obtain a more accurate model.

The model developed offers the possibility of exploring the limits and capacities of the real system without the necessity of running experiments. Moreover, its versatility and modularity provide a good basis to encompass other integration steps and even the integration of the full MELiSSA loop in a single model.

Acknowledgements

First of all, I would like to express my sincerest gratitude to my supervisors, Francesc Gòdia and Enrique Peiro, for the constant support, guidance and help given to me throughout the development of my thesis.

I would like to offer my special thanks to Laurent Poughon for the invaluable assistance provided during my research, without which this project would probably not have been possible.

Additionally, I wish to acknowledge Olivier Gerbi and Jean François Cornet for solving significant issues encountered throughout this thesis.

I would like to thank again Francesc Gòdia, Laurent Poughon and also Gilles Dussap for offering me the opportunity of spending a few days at the UBP in Clermont Ferrand to gain more knowledge about the topic of my thesis.

I am particularly grateful for the encouragement and advice given to me by Mireia Sánchez and for always being on my side.

Last but not least, my special thanks are extended to my family for putting up with me no matter the circumstances.

Table of Contents

List of Figures

List of Tables

Glossary

CELSS	Controlled Ecological Life Support System
CIVa	Compartment IVa of the MELiSSA loop (*Arthrospira platensis*)
CV	Compartment V of the MELiSSA loop (Crew)
DNA	Deoxyribonucleic Acid
EPS	Exopolysaccharides
ESA	European Space Agency
ISS	International Space Station
(IS) WP	(Integration Strategy) Work Package
JAXA	Japan Aerospace Exploration Agency
MELiSSA	Micro-Ecological Life Support System Alternative
MPP	MELiSSA Pilot Plant
NASA	National Aeronautics and Space Administration
PBR	Photobioreactor
RNA	Ribonucleic Acid
UAB	Universitat Autònoma de Barcelona
UBP	Université Blaise Pascal
XA	Active Biomass

Nomenclature

C_p	Compensation point ($W \cdot m^{-2}$)
C_x	Biomass concentration ($g \cdot L^{-1}$)
D	Dilution rate (h^{-1})
DF	Dark fraction (dimensionless)
E_a	Absorption mass coefficient ($m^2 \cdot kg^{-1}$)
E_s	Scattering mass coefficient ($m^2 \cdot kg^{-1}$)
F	Flow rate ($L \cdot h^{-1}$)
F_r	Incident radiant energy ($W \cdot m^{-2}$)
G	Gas molar fraction (dimensionless)
J_r	Mean radiant energy ($W \cdot m^{-2}$)
K	Half saturation constant ($g \cdot L^{-1}$)
K_J	Light half saturation constant ($W \cdot m^{-2}$)
$\overline{K}$	Equilibrium constant (dimensionless)
k	Partition coefficient (dimensionless)
$k_L a$	Mass transfer coefficient (h^{-1})
L	Liquid concentration ($g \cdot L^{-1}$)
M	Molar mass ($g \cdot mol^{-1}$)
m	Mass (g)
$\hat{m}$	Mass flow rate ($g \cdot h^{-1}$)
N	Molar concentration ($mol \cdot L^{-1}$)
N^*	Molar concentration in saturation ($mol \cdot L^{-1}$)
n	Molar density ($mol \cdot L^{-1}$)
P	Total pressure (atm or mmHg)
PQ	Photosynthetic Quotient (dimensionless)

$\boldsymbol{p}$	Partial pressure (atm or mmHg)
$\boldsymbol{R}$	Cylindrical reactor radius (m)
$\boldsymbol{R_{il}}$	Illuminated radius (m)
$\boldsymbol{\widehat{R}}$	Reaction rate ($g \cdot h^{-1}$ or $mol \cdot h^{-1}$)
$\boldsymbol{\overline{R}}$	Ideal gas constant ($L \cdot atm \cdot K^{-1} \cdot mol^{-1}$)
$\boldsymbol{RQ}$	Respiratory Quotient (dimensionless)
$\boldsymbol{r}$	Radius (m)
$\boldsymbol{r_x}$	Volumetric rate of biomass production ($g \cdot L^{-1} \cdot h^{-1}$)
$\boldsymbol{S}$	Substrate concentration ($g \cdot L^{-1}$)
$\boldsymbol{T}$	Temperature (K or ºC)
$\boldsymbol{t}$	Time (h)
$\boldsymbol{V}$	Volume (L)
$\boldsymbol{x}$	Liquid molar fraction (dimensionless)
$\boldsymbol{y}$	Gas molar fraction (dimensionless)

Greek letters

$\boldsymbol{\gamma}$	Illuminated fraction of the reactor (dimensionless)
$\boldsymbol{\mu}$	Specific growth rate (h^{-1})
$\boldsymbol{\mu_{max}}$	Maximum specific growth rate (h^{-1})
$\boldsymbol{\nu}$	Stoichiometric coefficient (dimensionless)
$\boldsymbol{\chi}$	Molar fraction (dimensionless)

Superscripts and subscripts

$\boldsymbol{ap}$	Apparent
$\boldsymbol{cons}$	Relative to the consumption in a system
$\boldsymbol{EPS}$	Relative to the exopolysaccharides

$\boldsymbol{G}$	Relative to the gas phase
$\boldsymbol{G/L}$	Relative to the gas-liquid mass transfer
$\boldsymbol{gen}$	Relative to the generation in a system
$\boldsymbol{i}$	Relative to a component i
$\boldsymbol{in}$	Relative to the input of a system
$\boldsymbol{L}$	Relative to the liquid phase
$\boldsymbol{out}$	Relative to the output of a system
$\boldsymbol{photo}$	Relative to the photosynthesis
$\boldsymbol{rc}$	Relative to reactor conditions
$\boldsymbol{resp}$	Relative to the respiration
$\boldsymbol{S}$	Relative to a substrate S
$\boldsymbol{sc}$	Relative to standard ambient conditions
$\boldsymbol{XA}$	Relative to the active biomass

Chapter 1

INTRODUCTION

1.1. Life Support Systems in Space

The future of Space exploration is closely linked to the settlement of Mars, as a first step of a potential planetary colonization. The goal is clear but the challenges involved are huge. One of them is to maintain the crew alive for the whole duration of the mission. Since the Space environment is hostile for human life, there is a constant need for air, water, food and atmospheric control. Life support systems are in charge of the survivability of the human crew by means of four main functions: air revitalization, water reutilization, waste management and food production and preparation.

In order to carry on these tasks, a life support system can be divided depending on the means used (physicochemical or biological) and on the level of regeneration involved (regenerative and non-regenerative). Physicochemical systems are based on physical and chemical reactions to obtain metabolic consumables (e.g. oxygen production from water electrolysis), whereas biological systems rely on artificial ecosystems where biological reactions take place (e.g. photosynthesis of plants and other organisms). Finally, regenerative and non-regenerative systems are related to the capacity of a system to recycle and close (ideally) the loop not depending on external sources. Although biological systems offer a better auto-regenerative nature, they imply a huge launching mass and are less developed than physicochemical systems due to their high complexity. Studies have shown that, in terms of mass, biological systems become indispensable for long-term missions, but are not suitable for short ones (**Figure 1.1**). The last step of a totally closed system is called CELSS (Controlled Ecological Life Support System) and, conceived as a fully closed habitable artificial ecosystem, would be the last goal in terms of life support systems for long-range missions.

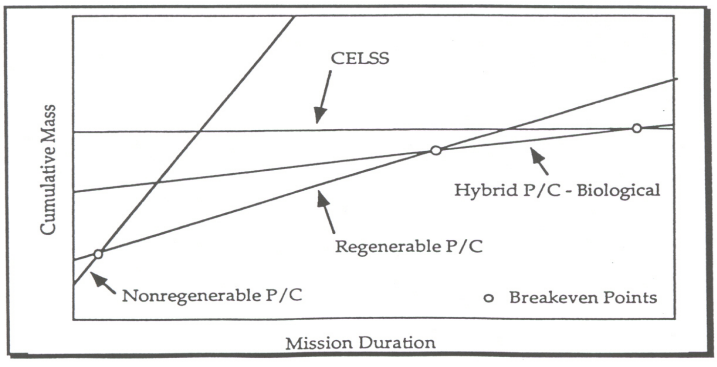

Figure 1.1 Cumulative launch mass according to different life support systems as a function of the mission duration

Nowadays, up to the ISS (International Space Station), the life support systems are all physicochemical (regenerative and non-regenerative) and imply a constant supply of provisions from Earth to the station. In the ISS air and water recycling are performed, but the production of food and the correct treatment of wastes cannot be done by physicochemical means. The case of Mars is different since it is a long-term manned Space mission. Due to the mission duration, a reliable life support system, including food supply and waste management must be considered. In terms of weight (launched and supplied mass of metabolic consumables), and hence cost, the use of biological life support systems is totally needed. The key of the biological systems is the production of food, requiring a concomitant the recycling of wastes (in addition to water and air). And for those long missions, resource recycling, ideally meaning the closure of gas, liquid and solid loops, is essential.

1.2. The MELiSSA Project

During the last decades, several Space Agencies including NASA, JAXA and ESA have been studying biological life support systems to maintain life during a long period of time out in Space, without the inconvenience (economical and technological) of resupplying continuously the mission from Earth for its whole duration. In Europe, this effort has been performed primarily within the MELiSSA project, which stands for Micro-Ecological Life Support System Alternative. MELiSSA is conceived as the first step towards the future development of regenerative life support systems for long-term manned missions, starting from basic research and development studies up to a comprehensive ground demonstration of the technologies developed.

The MELiSSA project is an international project leaded by ESA and developed by a Consortium of 13 partners, one of them being *Universitat Autònoma de Barcelona*. UAB joined the Consortium as a new partner in 1995, with its contribution focused on the hosting and developing the MELiSSA Pilot Plant (MPP) – Laboratory Claude Chipaux. The MPP is a facility created to demonstrate the MELiSSA loop in terrestrial conditions and to make it the primary European Facility for Life Support Ground-Demonstration. It is located at UAB, in the *Departament d'Enginyeria Química, Escola d'Enginyeria*.

The MELiSSA idea is based on the duplication of the Earth functions without benefiting from Earth's resources and from terrestrial comfort. The main objectives of MELiSSA are the recovery of food, water and oxygen from wastes, using light as a source of energy. Inspired by an aquatic ecosystem, MELiSSA loop is divided into five main systems or compartments, each one in charge of one specific function. This kind of compartmentalized structure is needed to simplify the whole system and the very high level of requirements in terms of robustness and safety. The basics of the MELiSSA concept are shown in **Figure 1.2**.

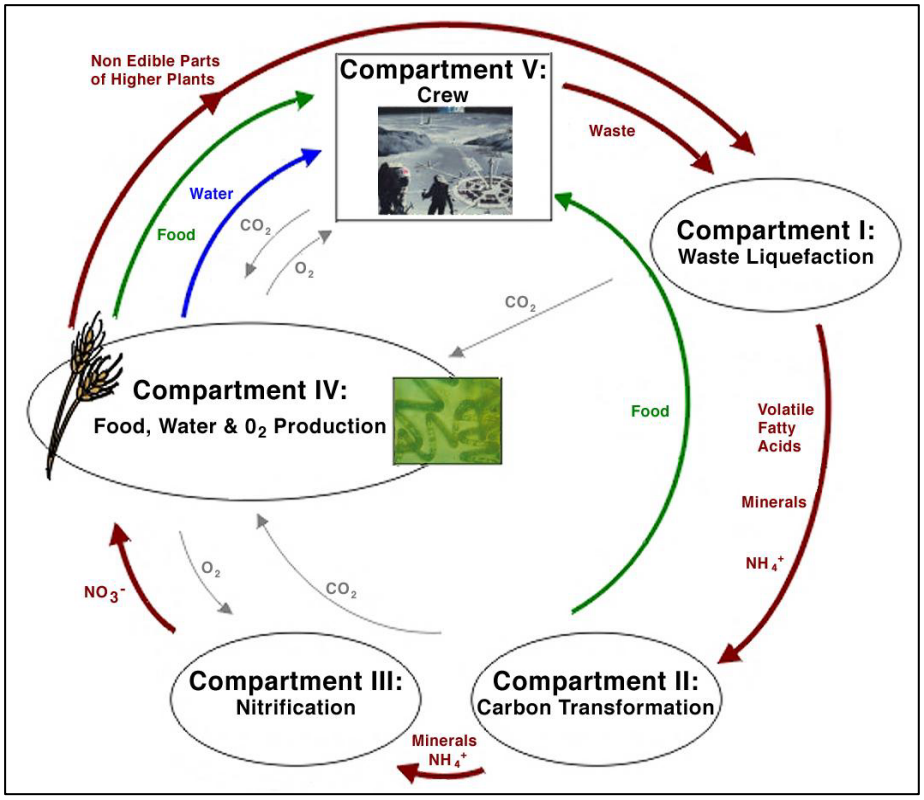

Figure 1.2 Compartmentalized structure of the MELiSSA loop

As a first step, each compartment has to be developed and characterized at individual level. As a final step, the five compartments must be integrated in closed loop in all their phases (gas, liquid and solid). The MELiSSA compartments will be integrated within the MPP, with the ultimate objective of a long-term demonstration (around one year of continuous operation) of the MELiSSA whole loop (the 5 compartments interconnected). Once this process is successfully done, the main goal of the MELiSSA Pilot Plant will be achieved.

It is important to notice that the five compartments are developed up to a pilot scale, according to a demonstration scenario defined by the MELiSSA Consortium. It consists of the production of oxygen for the equivalent of one-person respiration while producing at least 20% of the daily needed food. The closure of the MELiSSA loop will be carried out using animals as a mock-up of the crew compartment, in order to simplify the feasibility of the experiments in terms of economical cost and safety measures. The animals chosen are laboratory rats (Wistar rats), taking into account as a quantitative approach that 1 human is equivalent in terms of respiration to 40-60 rats.

To reach the final configuration, an approach strategy is defined. Initially, the work concentrates on the continuous operation of the compartments individually. At the same time, studies are made to develop the interfaces needed between compartments. Finally, the compartments are connected progressively, verifying the correct behavior of the system at each step of integration [1] [2].

1.3. Purpose and Methodology of the Work

The integration process between compartments, starting in 2015, will be done gradually, through different steps, called integration strategy work packages (IS WP). A roadmap of the integration steps is already configured (following the Integration Strategy of the MPP), being the WP1 the first to be accomplished. This first integration package is the main focus of this work and involves the gas loop closure between compartments CIVa and CV (**Figure 1.3**).

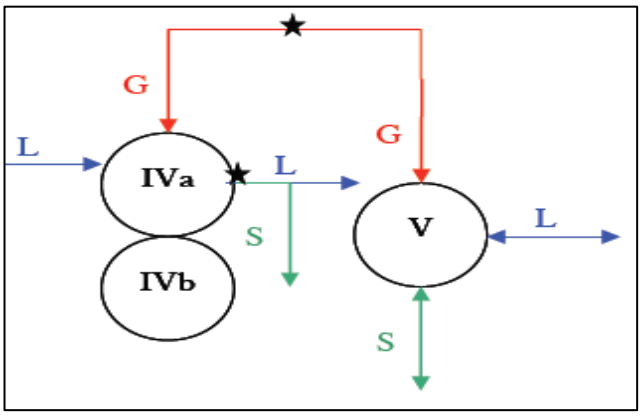

Figure 1.3 Closure gas phase CIVa - CV diagram

The main purpose of this thesis is to carry out a proper simulation for the integration WP1 experiment, using the software MATLAB/Simulink. The aims of the simulation are the following:

- To provide realistic data of the WP1 to be able to foresee how the system will behave depending on different working conditions and taking into account possible perturbations. Having a simulated model of the real experiment offers potential advantages in terms of exploitation of different system configurations.

- To compare, after the WP1 ends up, data from both the real and the simulated model, in order to find possible issues and to be able to optimize the model used for the simulation and its methodology.

- To serve as a basis for the next integration steps. Considering a modular simulation, the gradual implementation of the other compartments could be envisioned.

1.4. Outline of the Work

After a brief introduction, in Chapter 1, about life support systems in Space and the MELiSSA environment, Chapter 2 shows a more detailed view of the WP1, defining the experiment and the compartments CV and CIVa. The physical model associated

to the system is then described through the different processes involved, distinguishing between compartments.

Chapter 3 deals with the software definition of the model (MATLAB/SIMULINK), focusing specially on the Simulink interface and the main blocks used to perform the simulation.

Chapter 4 includes the results of the WP1 simulation and the comparison between them and the data obtained from the real integration experiment. Moreover, going a step further with the simulation tool, the manipulation of some operational variables is discussed and extra scenarios are simulated to find out the potential effects of those changes into the whole system.

Finally, Chapter 5 summarizes the results obtained throughout the project. In addition, this chapter contains the main conclusions that we can extract from the simulation tool and a personal point of view for future integration steps of the MELiSSA loop.

1.5. Motivation

Since I was a child, I have always been fascinated by the science and its mightiness. After thinking a lot, I found myself enrolling in aeronautical engineering, even though I was not really sure about my decision. Once I finished my Bachelor's degree, I realized that my real passion was the outer Space. This is the reason why I started the Master in Aerospace Science and Technology. By the time I had to choose the Master Thesis subject, most of the topics were directly related to telecommunications or materials and I was not really interested in them. At the same time, we had a subject called Life Support Systems in Space and I really loved it, probably because it was special and different from the others, probably because it made me feel much "closer to the Space". I found it also interesting because it dealt with chemistry and biological processes, and that was something I had almost forgotten from the high school. With all that, I tried to focus my Master Thesis on the life support systems in space and I felt lucky because I could finally do it and learn a lot about the chemical and biological processes involved, as well as the environment and complexities associated to a real engineering project like the MELiSSA Project.

Chapter 2

PHYSICAL MODEL DEFINITION

2.1. WP1 Description

2.1.1. WP1 Introduction

The WP1 consists in the connection of CIVa and CV in the gas phase. It is very significant because it is the first integration step and will pave the way to further ones up to the whole integration of the MELiSSA loop. WP1 will generate very relevant data in terms of compartment interaction, mass balancing, control capacity, stability and reliability among others.

The WP1 includes a certain amount of different-level objectives, being the main one the demonstration of the dynamics of the O_2/CO_2 gas loop closure, coping with the evolution of the behavior of the system (CIVa – CV) depending on the needs and maintaining at a constant level the O_2 concentration in CV. This demonstration has already been performed at laboratory scale (BIORAT project), manipulating the light of the photobioreactor to adjust the O_2 production levels of the cyanobacteria at certain values. Other defined objectives for the WP1 are the following [3]:

- To remove all contaminants in CV gas phase (from and to CIVa) by passive technology under a defined threshold.

- To demonstrate the operation of both compartments in integrated mode for a relevant period of time.

- To accomplish the requirements of tightness for the gas loop involved in the WP1 integration, in order to obtain relevant data from the gas phase dynamics (a minimum of 80% of the initial gas should be maintained after 4 weeks of continuous operation). This is in fact one of the most critical and challenging aspects, not only for WP1, but also for the complete MELiSSA loop.

It is important to consider that the whole MELiSSA concept is conceived as a first step to a closed life support for manned habitats. Therefore, for this integration step three different phases are envisioned, corresponding to three different proposed set points of O_2 molar fraction in CV (18, 21 and 23%). In a gas mixture, the molar fraction of a constituent included in a volume is defined as:

$$\chi_i = \frac{Number\ of\ molecules\ of\ the\ constituent\ i}{Total\ number\ of\ molecules} \quad \textbf{(2.1)}$$

It is a dimensionless ratio, which can be expressed in percentage or ppm (parts per million). At sea level, the standard air composition is summarized in **Table 2.1**.

Table 2.1 Standard air composition at sea level

Gas	Fraction (%)
Nitrogen	78.084
Oxygen	20.946
Argon	0.934
Carbon Dioxide	0.033
Inert Gases	0.003
Carbon Monoxide	$6 \cdot 10^{-6}$

Although standard conditions are related roughly to 21% O_2 in the air, the other levels are taken into account to gain more information from a wider operational range and also to mimic potential extreme scenarios (having in mind potential conditions out in space). Those set points are based on a standard applicable to ESA projects that comprises general information and considerations on atmosphere quality [4]. The following situations are specified:

- Comfort situation: Situation with an environment that provides the astronaut a feeling of well-being. There is no need to take specific precautions with respect to his atmospheric environment.

- Discomfort situation: Situation where, due to the deviation of one or more atmospheric conditions, some action is needed in order to restore the comfort situation and protect the astronaut (although the perception of well being is not necessarily altered in a discomfort situation).

- Survival situation: Extreme situation where the astronaut faces atmospheric conditions that may be hazardous. Immediate protection is needed and actions are needed to restore either a discomfort or a comfort situation.

Figure 2.1 shows the O_2 fraction as a function of the total pressure and the corresponding zones of the situations aforementioned. Considering a nominal pressure in CV of 1 atm (1013 hPa), although with a small overpressure (of the order of 200 Pa), the comfort zone is located at around 21% O_2. On the other hand, the limits of the discomfort zone are located roughly at 25% O_2 on the upper side and 17-18% O_2 on the lower side. Outside the limits of the discomfort zone, the survival zone defines extreme conditions. At 1013 hPa, O_2 fraction must be maintained below 25%, because of the risk of fire. Between 25% and 30% special precautions have to be taken until O_2 fraction below 25% is restored. Below 17% O_2, symptoms of hypoxia are induced due to the lack of O_2. Those symptoms range from loss of night vision to loss of consciousness and even death (anoxia) depending on the O_2 level.

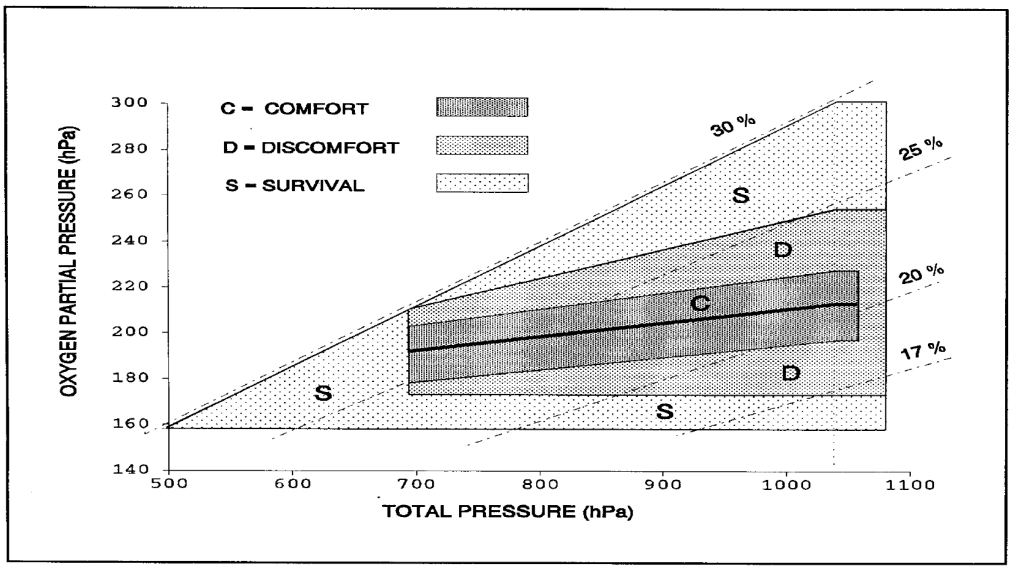

Figure 2.1 Oxygen partial pressure crew requirements

To encompass all potential scenarios inside the comfort and discomfort zones, the three O_2 fraction levels mentioned before (18%, 21% and 23%) are considered. For that reason, WP1 consists on three CIVa-CV gas loop integration phases, one for each CV O_2 setpoint (± 0.5% within the crew cabin atmosphere). In addition to these steps, a previous reference group testing of CV at 21% O_2 is considered (crew compartment in stand-alone operation with rats), making a total of 4 experimental phases with a group of 3 rats for each one.

For each of the integrated CIVa-CV phases, a specific sequence is followed (**Table 2.2**). Counting all 3 phases, the total duration of the WP1 is about 18 weeks (6 weeks for each phase) or 24 weeks if the reference group phase is taken into account [5].

Table 2.2 Operation sequence during the CIVa-CV gas loop integration phases

Sequence Number	CV Status	CIVa Status	Duration (days)
1	Quarantine	Stand-Alone	5
2	O_2 Adaptation	Integrated	4
3	Constant O_2	Integrated	28
4	Hardware/materials preparation*	Stand-Alone	5

*Includes removal of animals, cleaning, disinfection and materials preparation (cages, bedding, food)

2.1.2. Compartment V (Crew Compartment)

Compartment V is an animal isolator built by Hosokawa Micron LTD (UK) according to the requirements of the MPP, designed to provide a suitable living environment for rats and also to provide the necessary gas treatment systems in a recirculation loop to allow experiments to be carried out (**Figure 2.2**).

This compartment, with a total operational volume of around 1600 L, comprises an isolator main chamber and a transfer airlock for material/rats transfer into and out of the isolator. The isolator is a single chamber with a living area and a working area, which is used for transferring animals between cages, cleaning of cages, testing of animals, etc. All the operations in the isolator are carried out via gloveports located on the front of the isolator, allowing the monitoring and manipulation of the rats. Moreover, to ensure adequate environmental conditions for the animals, temperature, humidity, airflow, illumination photoperiod and gas composition are controlled and gas contaminant removal is also provided.

The isolator, made of stainless steel and fitted by laminated glass viewing windows, is specially built to meet high tightness constraints. The base system has the capacity of hosting up to 12 rats (6 cages with 2 rats each cage). Nevertheless, it is a modular system that can be extended by adding an additional chamber, providing up to 10 cages with a total of 20 rats [6].

The crew of compartment V is composed by Wistar rats, which consume the O_2 coming from compartment IV (only IVa in the case of WP1) and give back CO_2 as a product of their respiration.

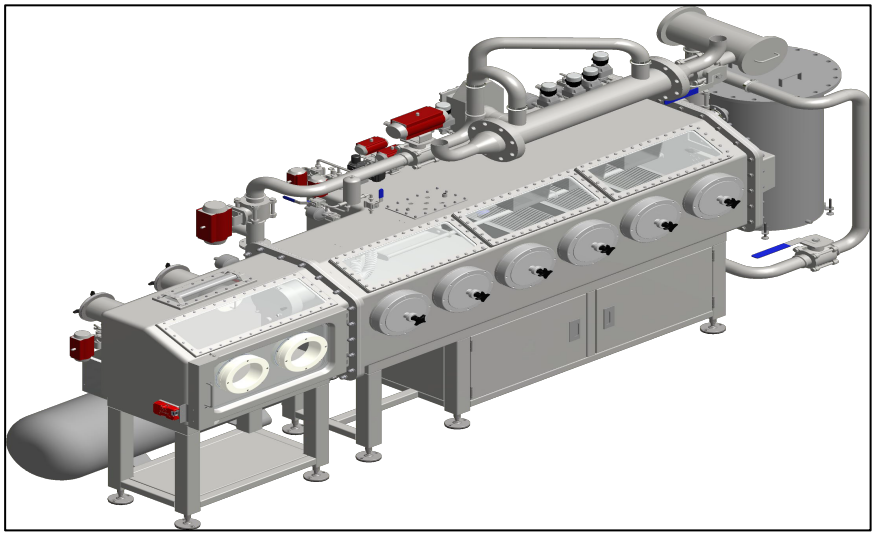

Figure 2.2 Compartment V of the MELiSSA Pilot Plant

2.1.3. Compartment IVa (Photobioreactor)

Built by the company De Dietrich Equipos Químicos, S.L (Spain), this compartment is based on a photosynthetic reactor (photobioreactor), which is shown in **Figure 2.3**. Designed in order to optimize the light distribution in the volume of the reactor, it is a stainless steel and glass external loop airlift photobioreactor with an operational volume of 83 L.

The illuminated part of the photobioreactor consists of two cylinders made of glass and 350 halogen lamps (OSRAM, 12 V, 20 W) distributed homogeneously around the cylinders. Both cylinders are connected at their lower and upper parts by U-shaped stainless steel sections, supporting all the valves and instrumentation (**Figure 2.3**, right). The instrumentation comprises various probes that allow on-line measurement of the main parameters of the culture (biomass concentration, pO2, pH, temperature, head pressure and outlet gas analysis) for control purposes [7].

CIVa is colonized by a culture of the cyanobacteria *Arthrospira platensis (*a.k.a. *Spirulina platensis).* Through the consumption of CO_2 and using light as energy source, this culture is able to provide both edible biomass and O_2 for the respiration of the crew (it can provide roughly 5% of the daily need of one human in O_2). Both biomass and O_2 production can be modulated by means of the regulation of the light supply to the culture, adapting the oxygen production to the specific demands of the crew.

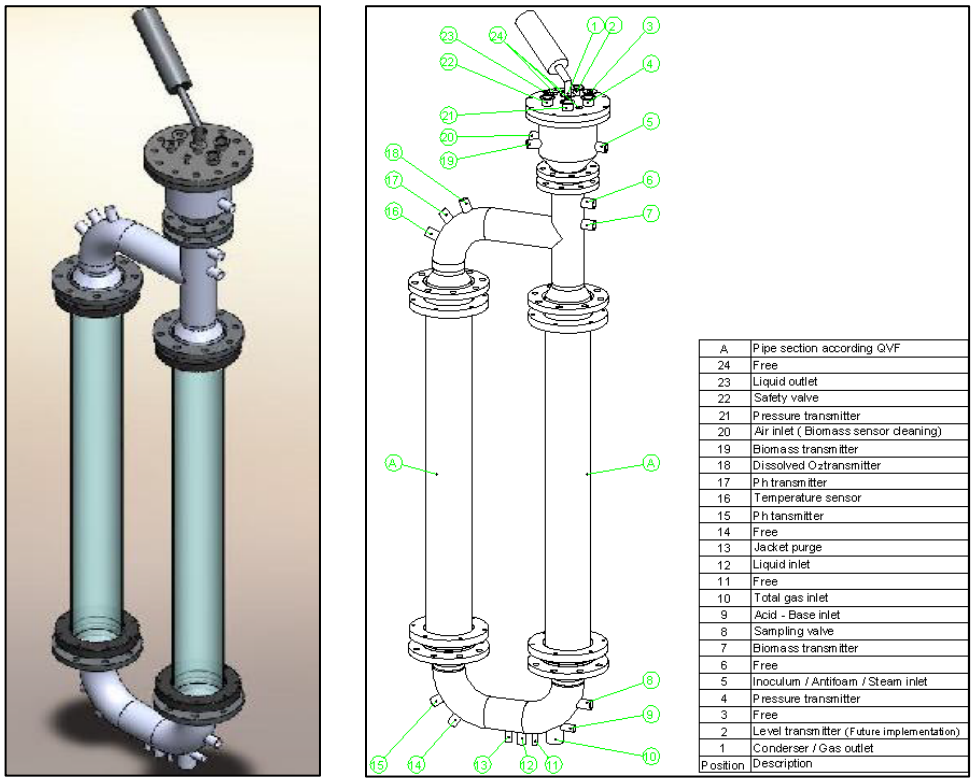

Figure 2.3 Compartment IVa of the MELiSSA Pilot Plant

2.1.4. WP1 Principles

The first integration between CIVa and CV relies on the gas phase loop, and more specifically on the dynamics established between two biological systems: the rats in CV and *Arthrospira platensis* in CIVa.

Starting from the crew compartment, rats consume O_2 at a given rate and produce CO_2, which goes into the photobioreactor. CO_2 is then transferred into the liquid phase of the PBR and dissolving in it (CO_2 (l)). By means of the photosynthesis, this CO_2 is consumed while O_2 is produced and then transferred from the liquid to the gas phase (O_2 (g)). Finally, the O_2 returns to the crew compartment and the loop proceeds again. Therefore, this whole loop encompasses three main processes: the respiration of the crew, the photosynthesis of the cyanobacteria and the gas/liquid exchange in the PBR. The schematics of this process can be seen in **Figure 2.4**.

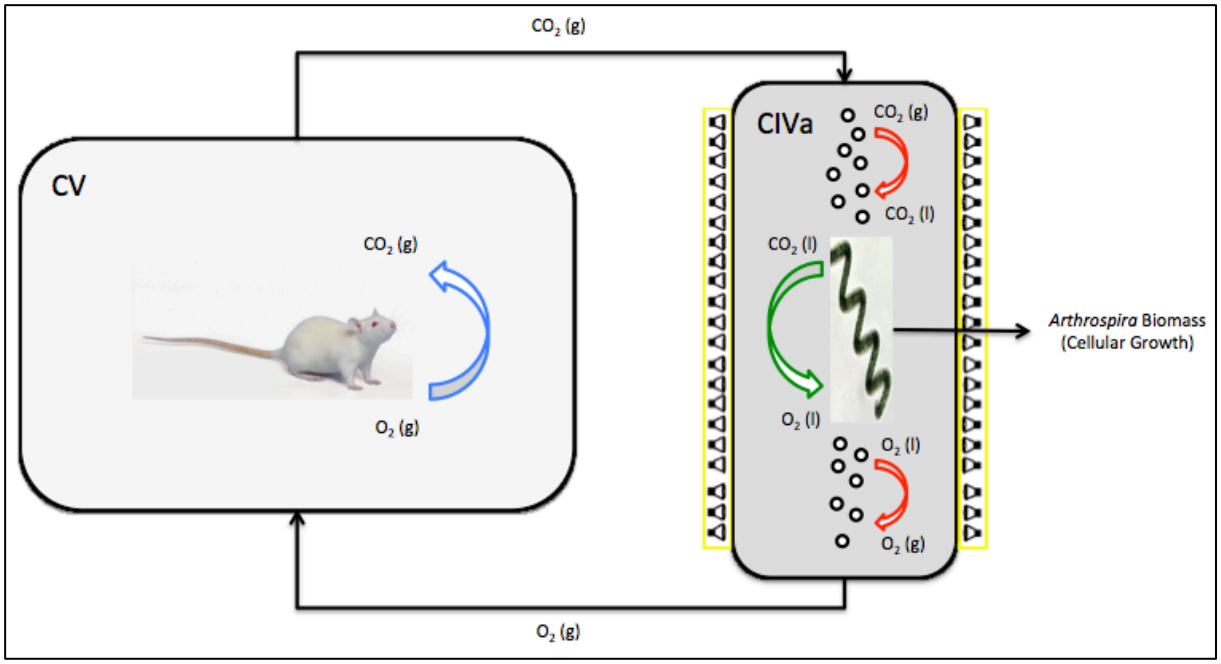

Figure 2.4 Schematics of the basic dynamics of WP1

To demonstrate the right performance of the closed loop, a suitable equilibrium (balance) between compartments has to be achieved. Even though the main focus is the gas phase, the liquid phase plays an important role in WP1 and has to be taken into account in the simulation. *Arthrospira platensis* is immersed and continuously fed by the liquid medium, described later on, which allows the culture to grow and perform its metabolic activities properly.

The mass balance of a system relies on its mass conservation during different physical and chemical processes. Considering $\dot{m}$ as the mass flow rate, the mass balance of any system can be defined as:

$$\frac{dm}{dt} = \left(\hat{m}_{in} + \hat{m}_{gen}\right) - \left(\hat{m}_{out} + \hat{m}_{cons}\right) \quad \textbf{(2.2)}$$

Or:

$$\frac{dm_i}{dt} = \hat{m}_{i_{in}} - \hat{m}_{i_{out}} + \hat{R}_i \quad \textbf{(2.3)}$$

Where dm/dt is the accumulation of each compound involved and it is determined by the inputs and outputs of the different components in the gas or liquid phase (m_{in} and m_{out}); and $\hat{R}$, standing for the reaction rate of the compounds (positive for generation and negative for consumption).

For the crew compartment, all components are in gas phase and R is reduced to O_2 and CO_2, since they are the ones taking part in the respiration of the crew. The main parameter that relates the consumption and production of O_2 and CO_2 for the crew in CV is the Respiratory Quotient (RQ), a dimensionless parameter defined as:

$$RQ = \frac{CO_{2\,gen}}{O_{2\,cons}} \quad \textbf{(2.4)}$$

For the photobioreactor, both gas and liquid compounds are mixed and the transfer rate between the gas and the liquid phase has to be considered in the reaction term R, which can be positive or negative depending on the phase involved. Moreover, R has to take also into account the generation and consumption of compounds related to the culture photosynthesis (only in the liquid phase). Following the same process aforementioned, the Photosynthetic Quotient (PQ) is defined for the culture in CIVa as:

$$PQ = \frac{O_{2\,gen}}{CO_{2\,cons}} \quad \textbf{(2.5)}$$

In the case of the whole WP1 loop, the equilibrium between CIVa and CV depends briefly on the O_2/CO_2 gas rates (controlled mainly by the number and behaviour of the rats and the light provided to the cyanobacteria). In other words, the equilibrium between the two cultures is obtained when the product RQ and PQ equals to one. However, this is the ideal case and both quotients are very difficult to equilibrate in practice. When PQ and RQ do not compensate each other, problems may arise, being the CO_2 accumulation in the crew compartment a critical one (considering the system *Arthrospira*-Rats). Fortunately, CO_2 is transformed to O_2 in CIVa and also dissolved in liquid (CO_2 and ionic forms). In that sense, as a consequence of the non-closure of the liquid loop, part of the CO_2 is evacuated by the outlet liquid flow and it helps balancing CV with CIVa.

2.2. Crew Compartment (CV)

2.2.1. Crew Composition

The respiration process is produced in the crew compartment (CV), which is hosted by female Wistar rats (**Figure 2.5**), currently one of the most used rats for laboratory research. The animal was selected after a study made by experts in animal requirements and physiology considering the characteristics, the space and the O_2 production in the MPP [8]. Some of the average characteristics of the Wistar rats are listed in **Table 2.3**.

Table 2.3 Wistar rats average characteristics

Parameter	Average Range
Adult Body Weight (g)	180-350
Temperature (ºC)	20-26
Relative Humidity (%)	45-65
Life Span (yr)	2-3
Food Consumption ($g \cdot day^{-1}$)	10-40
Photoperiod (light/dark)	12/12-14/10

To carry out the WP1 integration, 3 female Wistar rats for each phase with a life span of 14 to 30 weeks is selected (simulating humans with 20-50 years), and a day/night cycle of 12 hours is considered. It is significant to know that Wistar rats are nocturnal animals, which means a highest O_2 consumption during the night.

From the point of view of the feeding, there is no restriction to the food intake (*ad libitum* fed). To mimic space travel conditions and preserve the animal health, a balanced diet formed by 14.5% proteins, 61.5% carbohydrates and 2.6% fat is selected.

Figure 2.5 Wistar rat

2.2.2. Respiration Process

At a cellular level, respiration is the biochemical process of oxidising metabolites with oxygen, which produces energy, carbon dioxide, water and nitrogen compounds (this energy is required for thermal balance, motion, tissue renewal and growth). The respiration of the crew is the process that drives the dynamics of O_2 and CO_2 in CV. Both crew O_2 consumption and CO_2 production rates depend on several factors, being the most significant the specific diet, the body weight, the environmental variables (temperature, humidity, etc.), the day/night cycle and the animal activity.

The respiratory behaviour of the rats in the isolator was measured in the MPP prior to the official WP1 integration. The results obtained showed, considering the three rats, an average O_2 consumption of the order of 1.5 $g \cdot h^{-1}$ (0.047 $mol \cdot h^{-1}$) during the day and 2.5 $g \cdot h^{-1}$ (0.078 $mol \cdot h^{-1}$) at nights, each of the periods lasting for about 12 hours. Due to the noticeable difference between the day and night in terms of respiration rates, two metabolic states can be considered for the crew (Active/Inactive), each of them lasting 12 hours and taking into account that Wistar rats are nocturnal animals (they are active during night, which means that there is a higher O_2 consumption).

Results also demonstrated a fixed RQ of 0.98 no matter the period of the day. This result might appear strange, since RQ is often linked to the “activity” of the animal. However, this quotient is also dependent on the diet and this factor may lead to the constant and high RQ measured.

2.2.3. CV Mass Balance

From equation (2.3) and considering that gas compounds are described in terms of molar fractions, the gas balance in the crew compartment is defined by:

$$\frac{dG}{dt} = \frac{(G_{in} - G_{out}) n_{sc} F_G + \hat{R}_{resp}}{n_{rc} V_G} \tag{2.6}$$

Where G is the gas molar fraction of each compound and F_G is the gas flow rate (it is assumed that gas flow is the same at the input and output). $\hat{R}_{resp}$ encompasses the molar respiration rates as described in the section before. V_G stands for the total gas volume (i.e. the cabin volume in the case of CV) and n is the molar density taking into account specific conditions (standard ambient conditions and reactor conditions). The number of moles can be extracted from the ideal gas law:

$$n = \frac{P}{\bar{R}T} \tag{2.7}$$

With P belonging to the total pressure in atm, T the temperature in Kelvin and $\bar{R}$ the universal gas constant ($\bar{R}$ = 0.08206 $L \cdot atm \cdot K^{-1} \cdot mol^{-1}$).

2.3. Photobioreactor (CIVa)

2.3.1. Description of the Culture (*Arthrospira platensis*)

The culture selected for the photobioreactor in CIVa is the cyanobacteria *Arthrospira platensis*, known as *Spirulina* (**Figure 2.6**). A model based approach to optimize light transfer energy and biomass productivity has been adopted within MELiSSA. *Arthrospira platensis* is a photoautotrophic microorganism, since its primary energy source is the light and its primary carbon source is the inorganic carbon present as CO_2 in the atmosphere or as carbonate or bicarbonate ions in the culture media. It has high photosynthetic efficiency, low duplication time, high nutritional quality and value and non-toxic effect. Also, its low volume requirements to grow make this culture suitable for a closed ecosystem such as MELiSSA [9].

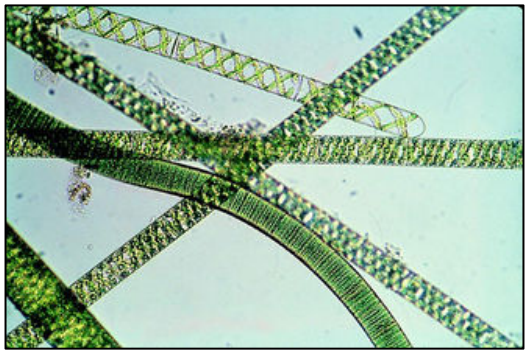

Figure 2.6 Arthrospira platensis (Spirulina)

The highly valuable nutritional properties of cyanobacteria like *Arthrospira platensis* are very important in bioregenerative life support systems. It is characterized, in optimal growth conditions (between 35-37ºC, with pH values around 9.5) [10], by high protein content (60-70% of its biomass), whereas the carbohydrates and the lipids represent 5-16% and 4-14% of its biomass respectively. The nucleic acid content is reported to be between 4-6% (approximately 78% RNA and 22% DNA). Finally, *Arthrospira* contains a high amount of vitamins such as A and B_{12} [11].

2.3.2. Photosynthesis Process

The photosynthesis is a physicochemical process by which photosynthetic organisms, such as cyanobacteria and higher plants, convert light energy into chemical energy. This process includes roughly the consumption of CO_2, H_2O, minerals and light and the production of O_2 and energy-rich organic compounds.

At an elemental level, the main elements that occur naturally in living systems are carbon, hydrogen, oxygen, nitrogen, phosphorous and sulphur (CHONPS). Those chemical elements are combined at molecular level to form the constituent macroelements of *Arthrospira platensis.* At the highest level, the biomass of the

Arthrospira platensis can be taken as the sum of two different compounds, each of them having their own stoichiometric equation: the active biomass (XA) and the exopolysaccharides (EPS). The active biomass is the amount of a given culture that is actively growing and it is mainly formed of proteins, lipids, carbohydrates and nucleic acids. On the other hand, the exopolysaccharides are compounds secreted by the culture into the surrounding environment.

The culture is cultivated in the photobioreactor in suspension in a Zarrouk culture medium [12] optimized by Cogne [13], whose main compounds are listed in **Table 2.4**. Despite the large amount of elements in the medium, only the main elements (CHONPS) are taken into account for the simulation, since they are the most representative to study the processes involved in WP1. In addition, to encompass the compounds used in the WP1 model (see Chapter 3), the medium is redefined as presented in **Table 2.5**. It is important to notice that, during the integrated phase, only CO_2 coming from CV is used as carbon source for the culture.

Table 2.4 Main components of the Zarrouk medium modified by Cogne

Compound	Concentration ($g \cdot L^{-1}$)
K_2HPO_4	0.50
$NaHCO_3$	10.50
Na_2CO_3	7.60
$NaNO_3$	2.50
K_2SO_4	1.00
NaCl	1.00
$MgSO_4 \cdot 7H_2O$	0.08
$CaCl_2 \cdot 2H_2O$	0.04
$FeSO_4 \cdot 7H_2O$	0.01
$EDTA \cdot 2H_2O$	0.09

Table 2.5 Main components of the simplified Zarrouk medium used for the model

Compound	Concentration ($g \cdot L^{-1}$)
HNO_3	1.9
H_3PO_4	0.3
H_2SO_4	0.6

From the active biomass and the EPS, a two stoichiometric equations model was obtained [14]. With all these considerations, the overall chemical reaction (stoichiometric equation) of the photosynthesis for the active biomass can be specifically written as:

$$CO_2 + 0.673\,H_2O + 0.192\,HNO_3 + 0.005\,H_2SO_4 + 0.006\,H_3PO_4 \xrightarrow{light} 1.444\,O_2 + CH_{1.566}O_{0.405}N_{0.192}S_{0.005}P_{0.006} \quad \textbf{(2.8)}$$

And for the exopolysaccharides:

$$CO_2 + 0.81\,H_2O + 0.015\,H_2SO_4 \xrightarrow{light} 0.96\,O_2 + CH_{1.65}O_{0.95}S_{0.015} \quad \textbf{(2.9)}$$

It is important to notice that the elemental balance of *Arthrospira platensis* is fixed by the stoichiometric coefficients in the previous equations, whereas the specific composition rates of active biomass and exopolysaccharides are linked to the specific growth of the culture.

2.3.3. Culture Growth Kinetics

The growth of a culture such as *Arthrospira platensis* is defined by its specific growth rate μ, and described by the following equation:

$$r_x = \mu C_x \quad \textbf{(2.10)}$$

where C_x is the biomass concentration, and r_x is the volumetric rate of biomass production. However, the specific growth rate of the biomass depends on the concentration of existing substrates in the culture media. Sometimes a specific substrate, called growth-limiting substrate, controls the growth kinetics. In the case of the growth of the cyanobacteria in CIVa, the limiting substrates are usually the CO_2 and light. To evaluate the effect of the different substrates on μ, the *Monod equation* is used:

$$\mu = \mu_{max} \frac{S}{K_S + S} \quad \textbf{(2.11)}$$

In this equation, μ_{max} is the maximum specific growth rate, S is the growth-limiting substrate concentration and K_S is the substrate saturation constant or half saturation constant. For high substrate concentrations ($S \gg K_S$) the specific growth rate is at a maximum level and it decreases as S decreases. Considering μ_{max} and K_S intrinsic values of the system cell-substrate, the relation between μ and S is showed by the Monod curve in **Figure 2.7**.

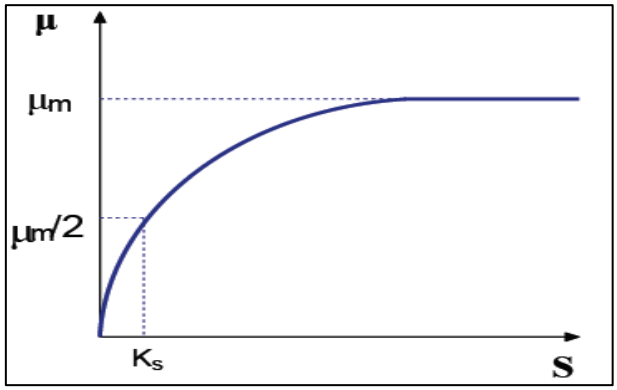

Figure 2.7 Culture specific growth rate as a function of substrate concentration

When more than one substrate is affecting the growth of the culture, as it is in the studied case, the Monod equation can be expanded as follows:

$$\mu = \mu_{max} \frac{S_1}{K_{S_1} + S_1} \cdot \frac{S_2}{K_{S_2} + S_2} \cdot \ldots \frac{S_n}{K_{S_n} + S_n} \quad \textbf{(2.12)}$$

For culture growth, the main limiting substrates are light (described in the next section) and CO_2. Although no consistent information about the CO_2 limitation in *Arthrospira platensis* is available, literature about other microalgae such as *Chlorella* sp. and *Synechocystis* sp. [15] and *Nannochloropsis salina* [16] show a K_{CO_2} of the order of 10^{-4}-10^{-5} g·L^{-1}, which can be reasonably used for our purposes. The influence of different CO_2 saturation constants on *Arthrospira* growth (for low CO_2 concentrations) is displayed in **Figure 2.8**.

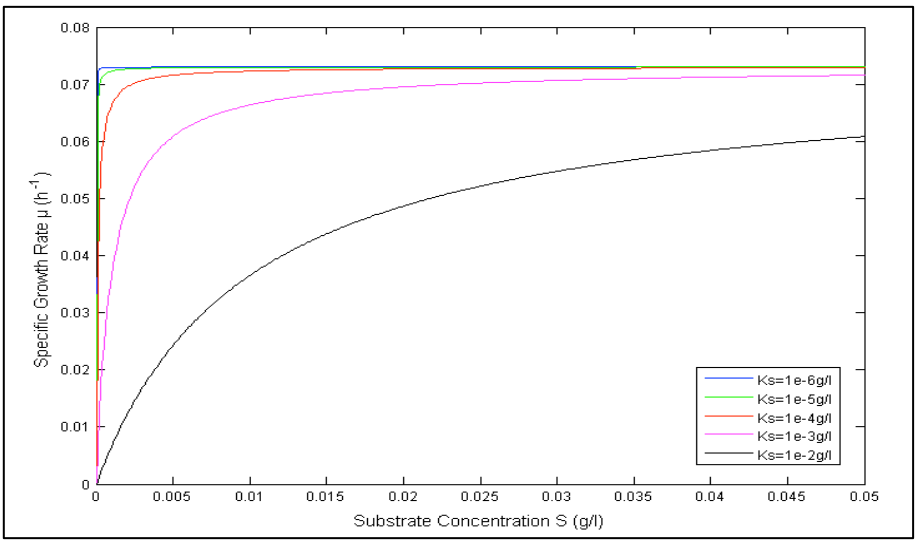

Figure 2.8 *Arthrospira platensis* specific growth rate for different CO_2 saturation constants (with $\mu_{max} \approx 0.073$ h^{-1})

2.3.4. Light Transfer Model and Coupling with Culture Growth Kinetics

Although the photosynthesis can be affected by several limiting substrates, the light intensity is the main variable to be considered. By changing this controlled variable, the O_2 produced by the cyanobacteria can be modulated according to the specific needs (within a limited range). Therefore, to establish a suitable light model, is indispensable to be able to analyse accurately the system.

The light model used was developed by J.F. Cornet [17] [18] and is specifically conceived for cylindrical photobioreactors, considering that the main limiting factor is light. It correlates the profile of light radiant energy $4\pi J_r$ in the PBR with the incident radiant light flux F_r (or light intensity) at its external surface, both in W·m^{-2}:

$$\frac{4\pi J_r}{F_r} = 2\frac{Bessel(0,r)\delta r}{Bessel(0,r)\delta R + \alpha Bessel(1,r)\delta R} \tag{2.13}$$

Where

$$\alpha = \left(\frac{E_a}{E_a + E_s}\right)^{1/2} \tag{2.14}$$

$$\delta = [E_a(E_a + E_s)]^{1/2} C_x \tag{2.15}$$

The light radiant energy is calculated as a function of the radius r and it takes into account the external radius R of the PBR, also known as the characteristic length of the PBR $(0 < r < R)$. E_a and E_s are the mean coefficient of absorption and scattering of the cell culture, while C_x stands for the biomass concentration. The light distribution profile derived from this model is shown in **Figure 2.9**.

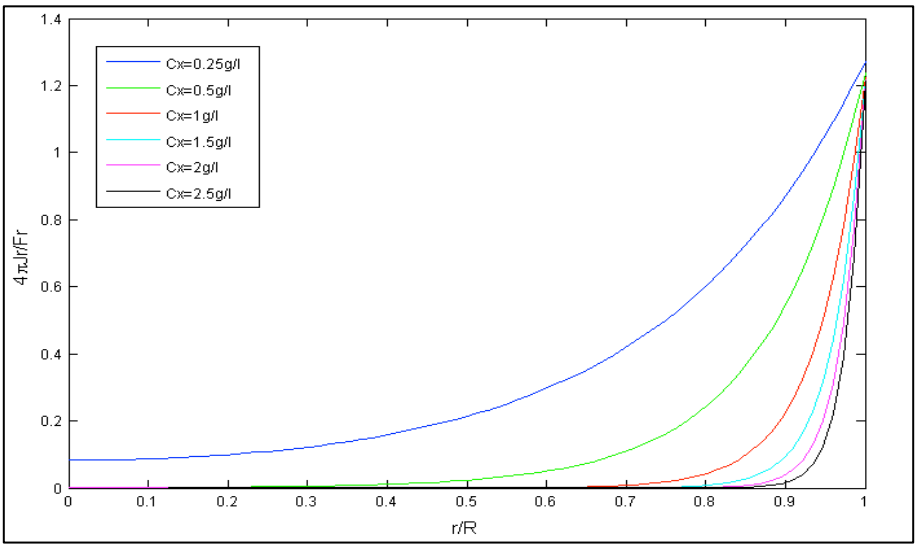

Figure 2.9 Light distribution profile vs PBR radial dimension for different biomass concentrations

To accurately model a PBR, the coupling between growth kinetics of the culture and the phenomena of light transfer is required. Following the Monod equation, the kinetic equation under light limitation takes the following formulation:

$$r_x = C_x \frac{\mu_{max}}{\pi R^2} \int_{R_{il}}^{R} 2\pi r \frac{4\pi J_r}{K_J + 4\pi J_r} dr \quad \textbf{(2.16)}$$

where K_J is the saturation constant for light and R_{il} is the illuminated radius of the PBR. It delimits the volume of the reactor having radiant energy levels above the compensation point C_p, at which photosynthesis becomes inefficient (1 W·m^{-2} for *Arthrospira platensis*). R_{il} is obtained solving the following equation:

$$2 \frac{Bessel(0,r)\delta R_{il}}{Bessel(0,r)\delta R + \alpha Bessel(1,r)\delta R} - \frac{C_p}{F_r} = 0 \quad \textbf{(2.17)}$$

Taking into account the two-stoichiometry model (XA and EPS) and bringing together equations (2.11) and (2.16) in order to encompass both light and CO_2 limitations, the total kinetic equation is defined by:

$$r_x^{XA} = C_x^{XA} \mu_{max}^{XA} \frac{[CO_2]}{K_{CO_2} + [CO_2]} \frac{1}{\pi R^2} \int_{R_{il}}^{R} 2\pi r \frac{4\pi J_r}{K_J^{XA} + 4\pi J_r} dr \quad \textbf{(2.18)}$$

$$r_x^{EPS} = C_x^{EPS} \mu_{max}^{EPS} \frac{[CO_2]}{K_{CO_2} + [CO_2]} \frac{1}{\pi R^2} \int_{R_{il}}^{R} 2\pi r \frac{4\pi J_r}{K_J^{EPS} + 4\pi J_r} dr \quad \textbf{(2.19)}$$

$$r_x = r_x^{XA} + r_x^{EPS} \quad \textbf{(2.20)}$$

with μ_{max}^{XA} = 0.073 h^{-1}, μ_{max}^{EPS} = 0.3 h^{-1}, K_J^{XA} = 20 W·m^{-2} and K_J^{EPS} = 750 W·m^{-2} [14].

2.3.5. Gas/Liquid exchange in the PBR

The photobioreactor in compartment IVa is of multiphasic nature, with a gas phase bubbled in a liquid phase. Therefore, the transport of CO_2 from the gas to the liquid and O_2 from the liquid to the gas is one of the phenomena influencing its performance.

In the scenario envisioned, where the culture is immersed in a liquid media, the mass transfer between gas and liquid is very important, due to the need to provide O_2 to the cyanobacteria. Since liquid O_2 has to be delivered to the culture and gas CO_2 to the rats, both liquid to gas and gas to liquid transfers have to be studied.

The gas/liquid transfer of a component i is measured by its mass transfer rate $\widehat{R}_{G/L}$, following respectively the equation:

$$\hat{R}_{G/L} = k_L a(N_i^* - N_i)V \quad \textbf{(2.21)}$$

with $\hat{R}_{G/L}$ positive for a transfer from gas to liquid and negative the other way around. $k_L a$ is the mass transfer coefficient, an intrinsic parameter of the system calculated empirically that depends on parameters like the temperature, the bioreactor volume and the gas flow rate. For the bioreactor considered, $k_L a$ was experimentally measured in first study in 2000, although considering a slightly lower volume of CIVa photobioreactor (77 L) and a temperature of 36ºC [19]. Some years later, another tests were run in the MPP with a photobioreactor volume of 85 L and at room temperature [20]. Although real CIVa conditions refer to a temperature of 36ºC and a volume of 83 L, the temperature is the most significant parameter to calculate the $k_L a$. For this reason, and taking into account an initial gas flow rate for the WP1 of around 168 $L \cdot h^{-1}$ (2.8 $L \cdot min^{-1}$), a $k_L a$ value of 10.5h^{-1} is considered.

In equation (2.21), N_i is the current molar concentration of the component i in the specific phase (gas or liquid) and N_i^* is the molar concentration of i in saturation also in the specific phase. N_i^* is calculated from the partition coefficient k_i , a dimensionless parameter defined as the ratio of the concentrations of a compound in a mixture of two immiscible phases at equilibrium. These coefficients define the distribution of a given compound between the gas and liquid phases. In the case of the gas/liquid mass transfer in the PBR, k_i is assumed to be the ratio between the gas and the liquid molar fractions (equation 2.22). Therefore, a $k_i = 0$ means that the compound is only in the liquid phase, while a $k_i > 10^{10}$ means that the compound is only in the gas phase.

$$k_i = \frac{y_i}{x_i} \quad \textbf{(2.22)}$$

With the partition coefficient, equation 2.21 can be rewritten, for gas-liquid and liquid-gas transfer respectively, as:

$$\hat{R}_{G/L_L} = k_L a \left(\frac{N_{i_G}}{k_i} - N_{i_L}\right) V_L \quad \textbf{(2.23)}$$

$$\hat{R}_{G/L_G} = k_L a \left(N_{i_G} - N_{i_L} k_i\right) V_G \quad \textbf{(2.24)}$$

Partition coefficients are described as a function of the temperature. For gases dissolved in H_2O, k_i can be calculated through the solubility of the specific gas in the water (x_i), assuming a partial pressure for the gas of 1 atm:

$$k_i = \frac{1}{x_i} \quad \textbf{(2.25)}$$

$$ln\, x_i = A + \frac{B}{T^*} + C\, ln\, T^* \quad \textbf{(2.26)}$$

$$T^* = \frac{T}{100K} \tag{2.27}$$

where x_i is expressed as a molar fraction, T is the temperature in Kelvin and A, B and C are component-specific constants, which depend on the temperature. In the case of dissolved CO_2, the calculation of its solubility in water is expanded to:

$$ln\, x_i = A + \frac{B}{T} + C\, ln\, T + DT \tag{2.28}$$

On the other hand, for liquids, k_i is computed from the vapor gas pressure (p_i), the partial pressure of liquid vapor in a gas mixture in equilibrium with its condensed states (liquid or solid). It is given by the *Antoine Equation* (equation (2.30)), very useful for modeling saturation pressures of liquids and solids. Assuming that the activity of water remains equal to 1 (x_i=1), k_i is calculated by:

$$k_i = \frac{y_i P}{P} = \frac{p_i}{P} \tag{2.29}$$

$$log_{10}\, p_i = A - \frac{B}{T + C} \tag{2.30}$$

where p_i and P (total pressure in the gas phase) are in mmHg (760 mmHg = 1 atm), T in ºC and A, B and C are again specific temperature-dependant constants for each compound.

Table 2.6 lists the constants for the determination of the partition coefficients of the most significant compounds, taking into account the photobioreactor temperature (36ºC). **Figure 2.10** shows the k_i variation for a range of temperatures between 0ºC and 60ºC. The other compounds involved in the WP1 are supposed to remain only in the liquid or gas phase.

Table 2.6 Component-specific constants for k_i determination

Compound	A	B	C	D
Oxygen	-66.7354	87.4755	24.4526	-
Carbon Dioxide	-159.854	8741.68	21.6694	$-1.103 \cdot 10^{-3}$
Water	8.10765	1750.286	235	-

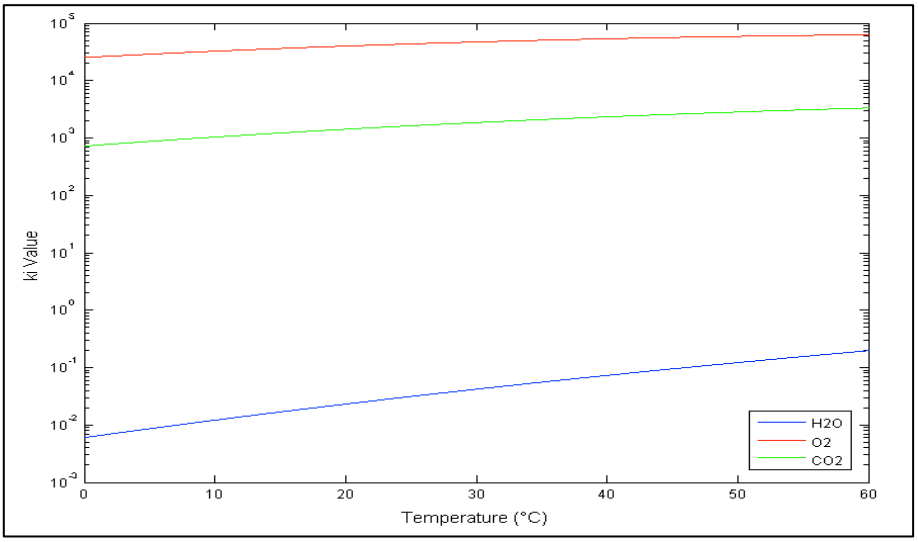

Figure 2.10 k_i variation as a function of the temperature for different compounds

For the case of CO_2, when describing the gas/liquid phase equilibrium, its ionic forms must be considered [21]. CO_2 dissolved in water decomposes into carbonic acid, bicarbonate and carbonate and the concentrations of these compounds depend on the pH value.

The equilibrium between carbonic acid and bicarbonate can be considered immediate, therefore only the reactions for bicarbonate and carbonate are taken into account. They can be written as:

$$CO_2 + H_2O \rightleftharpoons HCO_3^- + H^+ \quad \textbf{(2.31)}$$

$$HCO_3^- \rightleftharpoons CO_3^{2-} + H^+ \quad \textbf{(2.32)}$$

The equilibrium constants $\overline{K}$ of the reactions above and the correlations to calculate them as a function of the temperature (in Kelvin) are expressed by:

$$\overline{K}_1 = \frac{[HCO_3^-][H^+]}{[CO_2]} \longrightarrow ln\,\overline{K}_1 = \frac{-12092.1}{T} - 36.7816\,ln\,T + 235.482 \quad \textbf{(2.33)}$$

$$\overline{K}_3 = \frac{[CO_3^{2-}][H^+]}{[HCO_3^-]} \longrightarrow ln\,\overline{K}_3 = \frac{-12431.7}{T} - 35.4819\,ln\,T + 220.067 \quad \textbf{(2.34)}$$

Although the value of the partition coefficient is not affected by pH, pH modifies the quantity of total CO_2 dissolved in the medium. Therefore, pH affects the solubility of CO_2 and has to be considered and treated at the same step of the gas/liquid equilibrium. Considering an “apparent” solubility for the CO_2 compound (assuming bicarbonate and carbonate as an equivalent of CO_2 dissolved in a solution), a new partition coefficient is obtained:

$$k_{CO_2}^{ap} = \frac{y_{CO_2}}{x_{CO_2}^{ap}} \quad \textbf{(2.35)}$$

Instead of the real partition coefficient (equation (2.28)), a new "apparent" partition coefficient is considered for the total CO_2 gas/liquid equilibrium (CO_2 and ionic forms). The new partition coefficient takes into account both the temperature and pH and is related to the real partition coefficient by the equation below:

$$k_{CO_2}^{ap} = \frac{k_{CO_2} + y_{CO_2}\xi}{1 + \xi} \quad \textbf{(2.36)}$$

where

$$\xi = \frac{\overline{K}_1}{10^{-pH}}\left(1 + \frac{\overline{K}_3}{10^{-pH}}\right) \quad \textbf{(2.37)}$$

2.3.6. CIVa Mass Balance

The mass balance in the photobioreactor includes both liquid and gas balances, defined in terms of molar fraction and concentration respectively. From equation (2.3), the whole mass balance for each compound in the system is defined by:

$$\frac{dG}{dt} = \frac{(G_{in} - G_{out})n_{sc}F_G - \hat{R}_{G/L}}{n_{rc}V_G} \quad \textbf{(2.38)}$$

$$\frac{dL}{dt} = \frac{(L_{in} - L_{out})F_L + \left(\hat{R}_{photo} + \hat{R}_{G/L}\right)M}{V_L} \quad \textbf{(2.39)}$$

Most of the terms for the gas balance are already explained in section 2.2.3. L refers to liquid concentrations of the compounds inside the PBR, the same way that F_L is the liquid flow rate. V_G and V_L are in this case the gas and liquid volumes in CIVa and M stands for the molar mass of a compound.

$\hat{R}_{G/L}$ is the transfer rate term as described in the section before, which takes place only in the photobioreactor because of the gas/liquid mixing. Finally, $\hat{R}_{photo}$ encompasses the reaction rates derived from the photosynthesis, which are described by:

$$\hat{R}_{photo} = \left[\frac{r_x^{XA}}{M^{XA}}\left(\frac{\nu}{\nu_{XA}}\right)_{XA} + \frac{r_x^{EPS}}{M^{EPS}}\left(\frac{\nu}{\nu_{EPS}}\right)_{EPS}\right]V_L(1 - DF) \quad \textbf{(2.40)}$$

With ν being the stoichiometric coefficients of each compound involved in the active biomass and EPS chemical reactions (see section 2.3.2). r_x^{XA} and r_x^{EPS} are the

culture growth rates as defined in section 2.3.4 and DF stands for the dark fraction, the part of the reactor which is not illuminated due to the lack of lamps around (top and bottom of the reactor). It is assumed that around the 33% of the liquid volume of the photobioreactor is in the dark.

2.4. Control Law/System

To equilibrate the dynamics of CV and CIVa in integrated mode, for a relevant period of time, a control system is necessary. The main degrees of freedom of this closed loop are the number of rats and the light intensity in CIVa (F_r). Taking into account that the number of rats is fixed (3 rats), the main parameter that balances the demand and production of CO_2 and O_2 in both compartments is the light. Flow rates can also be manipulated, but they are in principle fixed by the conditions defined for the integration test.

Due to the specific illumination system (number and power of the lamps) and taking also into account the culture growth conditions of *Arthrospira platensis* in the CIVa, the incident light flux has to be within a specific range. In that sense, the range of illumination goes roughly from 20 $W \cdot m^{-2}$ to 225 $W \cdot m^{-2}$. The lower level constraint is due to the fact that it has been demonstrated that *Arthrospira platensis* cannot grow properly bellow 20 $W \cdot m^{-2}$ and the upper level is related to hardware limitations. Although 100% of the light capacity allows a total of 225 $W \cdot m^{-2}$, it has been proved that for values over 90% the effect of the light on the culture is negligible [18]. For that reason, light intensity in WP1 tends to be limited to 90% of its capacity.

The two main objectives of the control system developed for WP1 are the following:

- To maintain the O_2 concentration in the crew compartment at a constant level. For the purposes of WP1, those levels or set points are 18%, 21% and 23% in molar fraction, depending on the operating phase.

- To maintain the CO_2 level in the crew compartment below 2% (20000 ppm). Higher levels could be potentially toxic for the crew.

Up to now in the MPP, depending on the O_2 demands, the control system in CIVa adjusts the light intensity of the photobioreactor. Consequently, O_2 level is actively controlled. Nevertheless, CO_2 level is not controlled in the MPP, but studies have shown that for the specific working conditions of the WP1, CO_2 limit should not be reached.

Chapter 3

SIMULINK MODEL DESCRIPTION

3.1. Simulink WP1 Overview

The simulation of WP1 relies on the software Matlab/Simulink and was originally developed by Laurent Poughon, from the *Université Blaise Pascal* (UBP, Clermond-Ferrand, France). The simulation has been adapted considering the specific WP1 conditions. Moreover, a more suitable control module has been included according to that developed by Olivier Gerbi (*SHERPA Engineering,* La Garenne-Colombes, France).

Simulink ensures a mixture of graphic (user-accessible) environment and the code-programming domain. In that sense, the graphic interface offers the user a schematic global view of the CIVa-CV integration and the possibility to easily change the main parameters of the simulation from the specific dialog box or even from the simulation itself (temperature, pressure, pH, flow rates and composition, etc.). **Figure 3.1** shows the simulation interface, delimiting the three main modules of the system: the crew compartment, the photobioreactor and the control subsystem. The simulation is built using different Matlab functions and data, being the main Simulink file *MELISSA_CV_CIVa_WP1.mdl*. Nevertheless, S-functions are the core of the model, using differential equations to compute the dynamics of the WP1 loop. The code of this simulation is added at the end of this document and all the files used are provided as well. For a more detailed explanation about the algorithms and files used, refer to the MELiSSA TN 83.2: *Dynamic modelling of a coupled MELiSSA crew – compartment C4a with Matlab/Simulink* [22].

The dynamics of the simulation is extremely related to the mass balance between all the compounds in the loop. It is very important to mention that the model involves 23 compounds (**Table 3.1**), although the dynamic model of the gas closure phase between CIVa-CV does not depend on all of them. Those compounds where selected to allow the modular implementation of the other compartments of the MELiSSA loop into the simulation. For this reason, some of them are not taken into account for WP1 but are of paramount importance for the next integration steps.

Table 3.1 Numbered list of compounds in the simulation

1) H_2O	9) CO_2 and ionic forms	17) CH_4
2) NH_3	10) Acetic Acid	18) Inert Gas
3) H_2SO_4	11) Propionic Acid	19) Organic Matter
4) H_3PO_4	12) Butyric Acid	20) Nitrosomonas Biomass
5) HNO_3	13) Valeric Acid	21) Nitrobacter Biomass
6) HNO_2	14) Caproic Acid	22) Rhodobacter Biomass
7) Urea	15) N_2	23) *Arthrospira* Biomass
8) O_2	16) H_2	

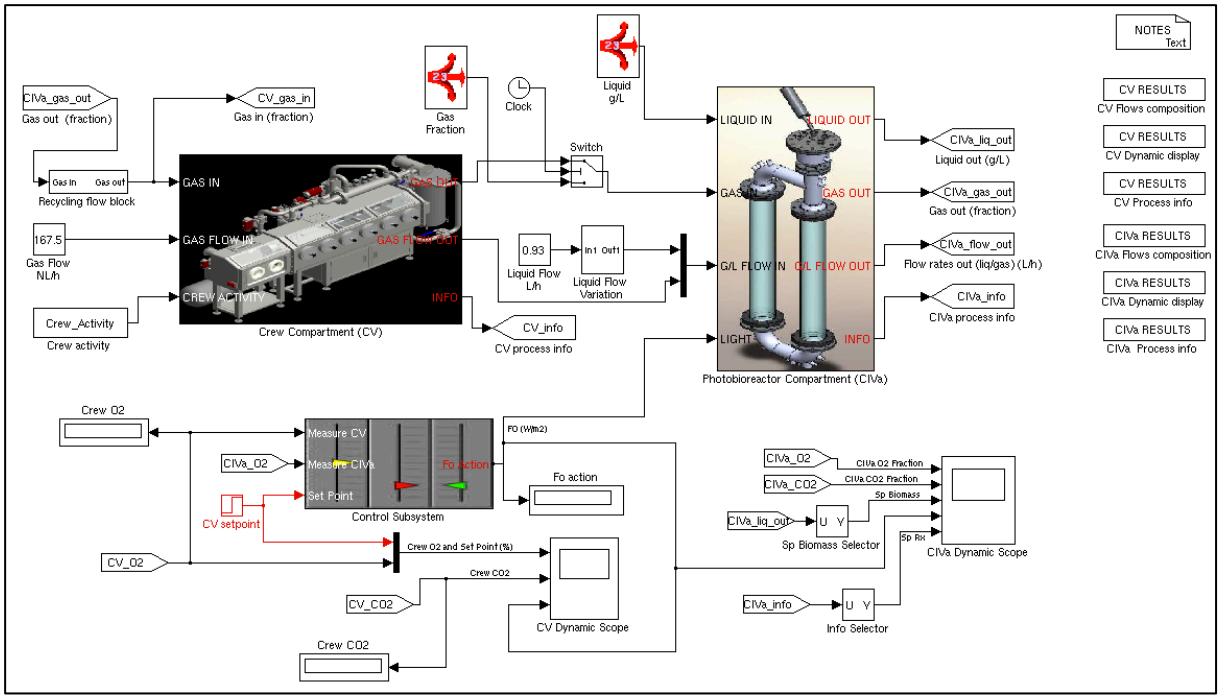

Figure 3.1 WP1 Matlab/Simulink interface

From **Figure 3.1**, the whole simulated loop can be summarized as follows: the gas flow coming from CIVa gets into CV, with a given flow rate and specific composition. After the respiration process in the crew compartment, which depends on the crew activity, the gas exits CV and flows through CIVa, which has a liquid feed (with its specific composition and flow rate) and a particular light intensity, regulated according to the control law. As a product of the dynamics on the photobioreactor, gas and liquid flows are released. Finally the gas enters CV and the loop starts again. Some important features to understand the basic loop shown in **Figure 3.1** are the following:

- Apart from gas/liquid composition and flow rates, other data are obtained from the dynamics of both compartments and are stored as process information (described in the next sections).

- All the information of gas and liquid flows and other parameters that evaluate the behaviour of both compartments and their dynamics are stored and can be monitored and observed from the boxes in the top right of the simulation interface.

- The most significant results of the simulation are directly shown in the Simulink interface. Crew O_2 and CO_2 and the light intensity action are displayed at each time step. Moreover, two scopes (for CV and CIVa) show the dynamic behaviour (for the whole time of simulation) of the most considerable factors involved in the WP1 loop.

- Both gas and liquid flow rates are assumed to remain constant for the whole loop (as an ideal case) for the simplicity of the simulation. Even though this

can be acceptable for the liquid phase, the assumption is less true when it comes to the gas phase, since the volume is more sensitive to the variation of the number of moles in the compartments.

- Since WP1 comprises only the gas phase closure, the liquid flow stays in open loop. This aspect is of paramount importance due to the fact that liquid flow contributes to wash out a certain amount of CO_2 in the liquid phase.

- External source gas/liquid composition can be accessed and changed from the boxes on top of the simulation interface.

- There is a switch that changes from an external gas flow source to the gas flow leaving CV at 48 hours. The reason for this is to avoid linking the crew with the photobioreactor when both compartments are not stabilized.

- A recycling flow block is added between the CIVa gas out and the CV gas in. It initializes the gas flow at time 0 and introduces a continuous delay of one calculation step in order to avoid algebraic loop difficulties.

3.2. CV Simulink Model

The dynamic CV model is based on the crew respiration, as well as the gas balance on the CV cabin. For this purpose, data obtained from the MPP about the metabolism of the rats are used. The CV block internal structure is shown in **Figure 3.2**, with the *CV_dyn* S-function being the core of it.

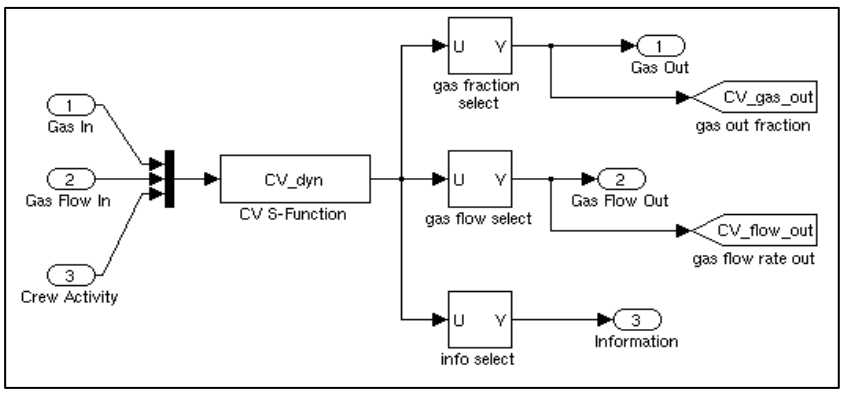

Figure 3.2 Simulink CV internal structure

The main inputs of the model are: the gas in flow composition for each compound (fraction), the gas in flow rate ($L \cdot h^{-1}$) and the code of the current crew activity (1:Active, 2:Inactive). On the other hand, the outputs are: the gas out flow composition for each compound (fraction), the gas out flow rate ($L \cdot h^{-1}$) and another CV process information. By default, this information includes the respiratory quotient

RQ, the O_2 consumption and CO_2 production rates ($g \cdot h^{-1}$) and the current activity code.

Moreover, crew compartment main parameters can be checked and changed, depending on the specific needs, from the CV dialog box (accessed by double-clicking the CV block. **Figure 3.3** shows the dialog box and the main crew compartment conditions used in the simulation. The user can choose also the number of rats, considering as a reasonable approximation that all rats have the same behaviour in terms of O_2 consumption and activities performed. If a more accurate model is needed, the user can redefine it and set specific data for each rat through the crew and planning definition files (**Table 3.2**).

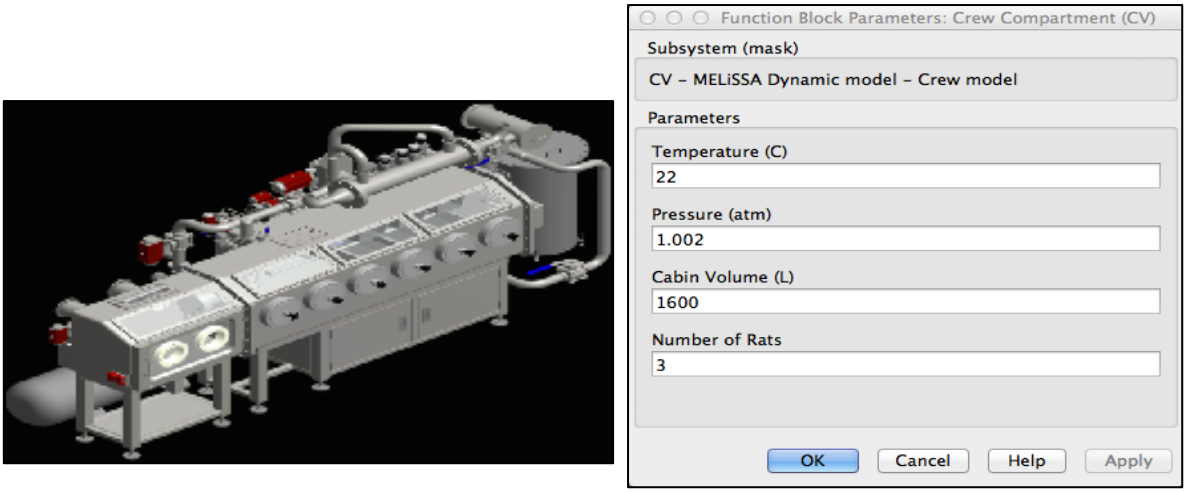

Figure 3.3 Crew compartment main block (left) and dialog box (right)

In addition to *CV_dyn,* other files are involved in the CV model. These files and their main functions are listed in **Table 3.2**. The overview of the CV algorithm with all the files involved is show in **Figure 3.4**.

Table 3.2 Additional files for the Matlab/Simulink crew compartment model

CV model files	Function
Crew_Activity.m	Calculation of the specific crew activity at each hour
crew_def.txt*	Crew definition: crew identifier and initial weight
planning.txt*	Crew planning definition: activity duration ($h \cdot day^{-1}$), activity code and crew identifier
calcul_crew.mat	Storage of process data from Crew_Activity.m
load_compounds.m	Definition of the WP1 compounds
calcul_CV.mat	Storage of process data from CV_dyn

*File not fully optimized due to the fact that the current simulation does not take into account a detailed description for each crew member and consider all members as a single block.

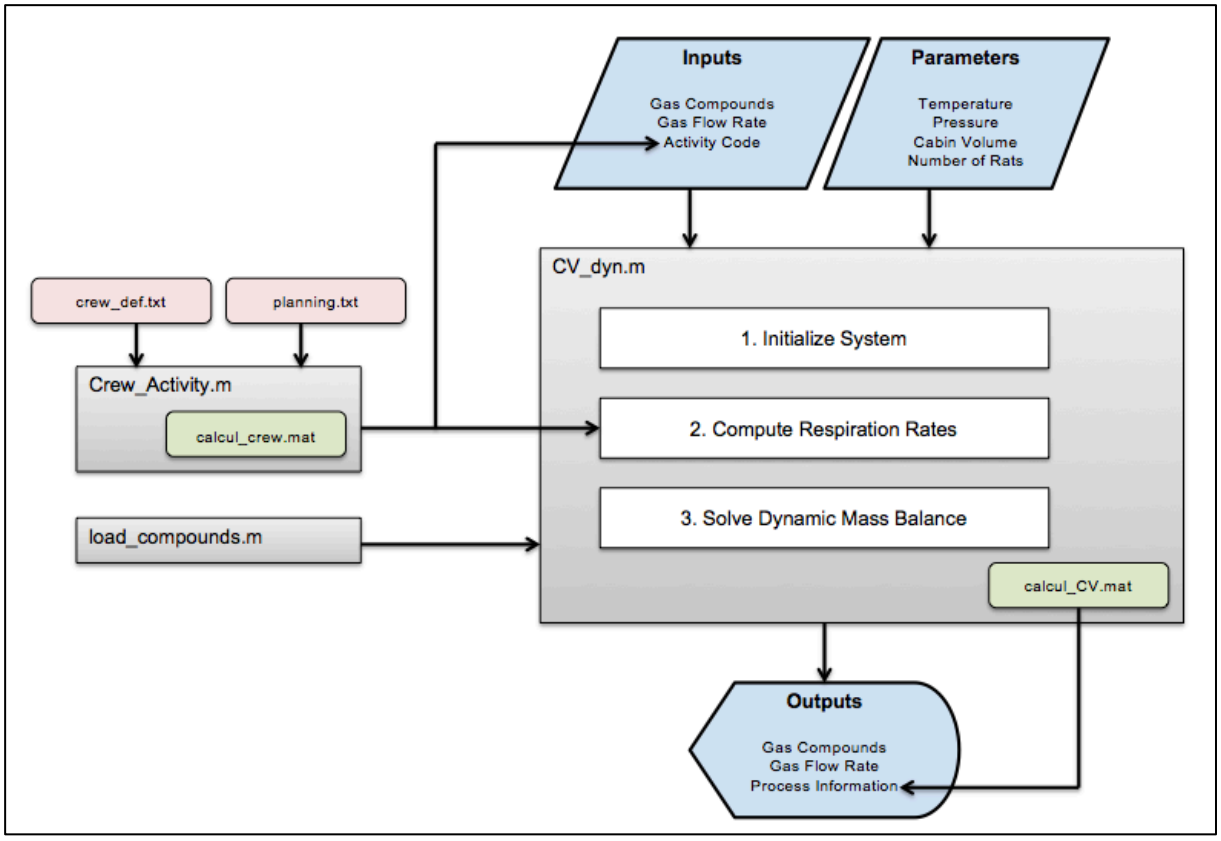

Figure 3.4 Simulink CV basic algorithm

3.3. CIVa Simulink Model

The CIVa model, based on the PHOTOSIM software, takes into account both the dynamic model of *Arthrospira* and the gas/liquid balance in the photobioreactor. The CIVa block internal structure is shown in **Figure 3.5**, with the *CIVa_dyn* S-function being the core of it.

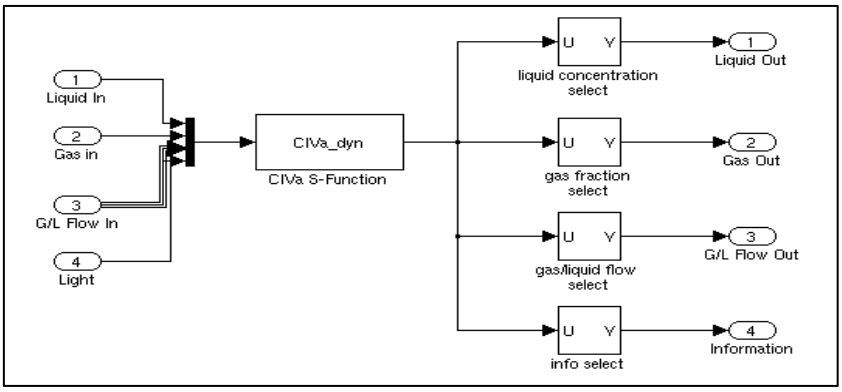

Figure 3.5 Simulink CIVa internal structure

The inputs of *CIVa_dyn* are: the liquid in flow composition for each compound ($g \cdot L^{-1}$), the gas in flow composition for each compound (fraction), the liquid and gas in flow rates ($L \cdot h^{-1}$) and the light Intensity ($W \cdot m^{-2}$). Finally, the outputs are: the liquid out flow composition for each compound ($g \cdot L^{-1}$), the gas out flow composition for each compound (fraction), the liquid and gas out flow rates ($L \cdot h^{-1}$) and other CIVa process information. By default, this information includes: the photosynthetic quotient *PQ*, the O_2 production rate ($g \cdot h^{-1}$), the cellular productivity r_x ($g \cdot L^{-1} \cdot h^{1}$), the illuminated fraction of the reactor γ, the substrate limiting factor and the dilution rate *D* (h^{-1}).

The user is again able to access and set the main CIVa process parameters from the dialog box by double-clicking the CIVa block. **Figure 3.6** shows the CIVa dialog box with the main reactor conditions used in the simulation. Three different reactor types with specific models can be selected: rectangular one side illumination, rectangular two sides illumination and cylindrical radial illumination. Furthermore, two different biological models for *Arthrospira platensis* can be chosen: single stoichiometric equation and two stoichiometric equations.

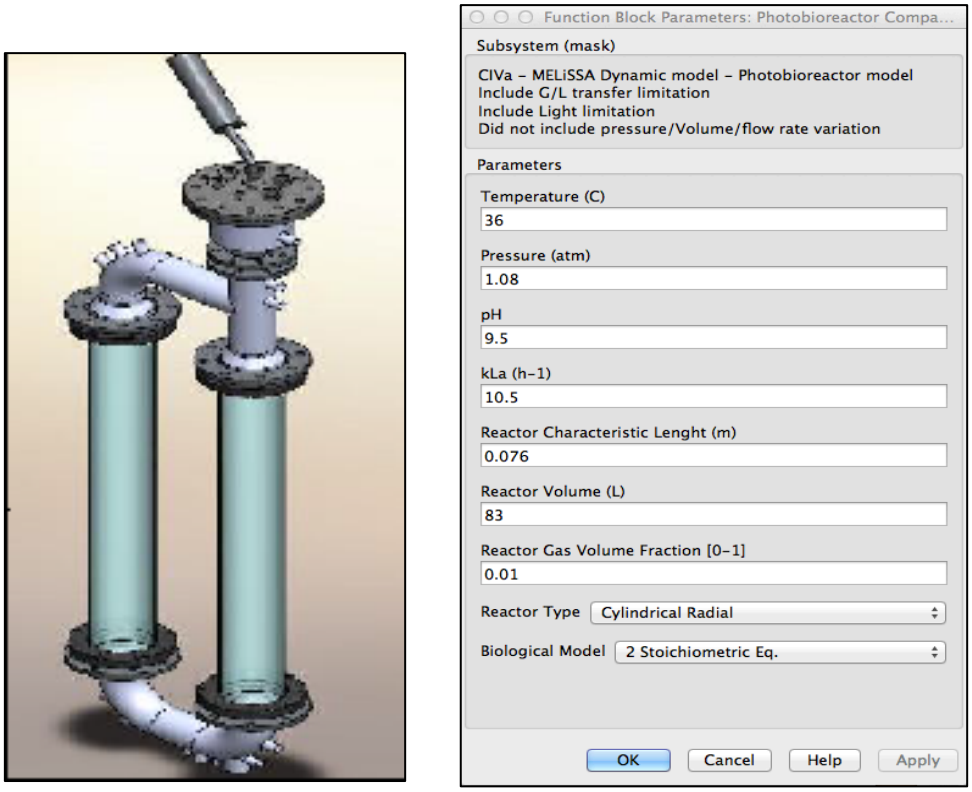

Figure 3.6 Photobioreactor main block (left) and dialog box (right)

Apart from the main function, the other files involved in the photobioreactor model and their main functions are listed in **Table 3.3**. The overview of the CV algorithm with all the files involved is show in **Figure 3.7**.

Table 3.3 Additional files for the Matlab/Simulink photobioreactor model

CIVa model files	Function
load_compounds.m	Definition of the WP1 compounds and their elemental composition
load_partitions.m	Definition of the partition coefficients for all compounds
composition_spiru.m	Definition of *Arthrospira* composition (based on the light provided)
composition_sp.mat	Storage of process data from composition_spiru.m
wil_reacteur.m	Calculation of the length of the reactor at which the light energy reaches the compensation point (R_{il})
wiv_reacteur.m	Calculation of the light profile structure that has to be integrated to estimate the culture growth rate ($\frac{2\pi r 4\pi J_r}{K_J+4\pi J_r}$)
calcul_CIVa.mat	Storage of process data from CIVa_dyn.m

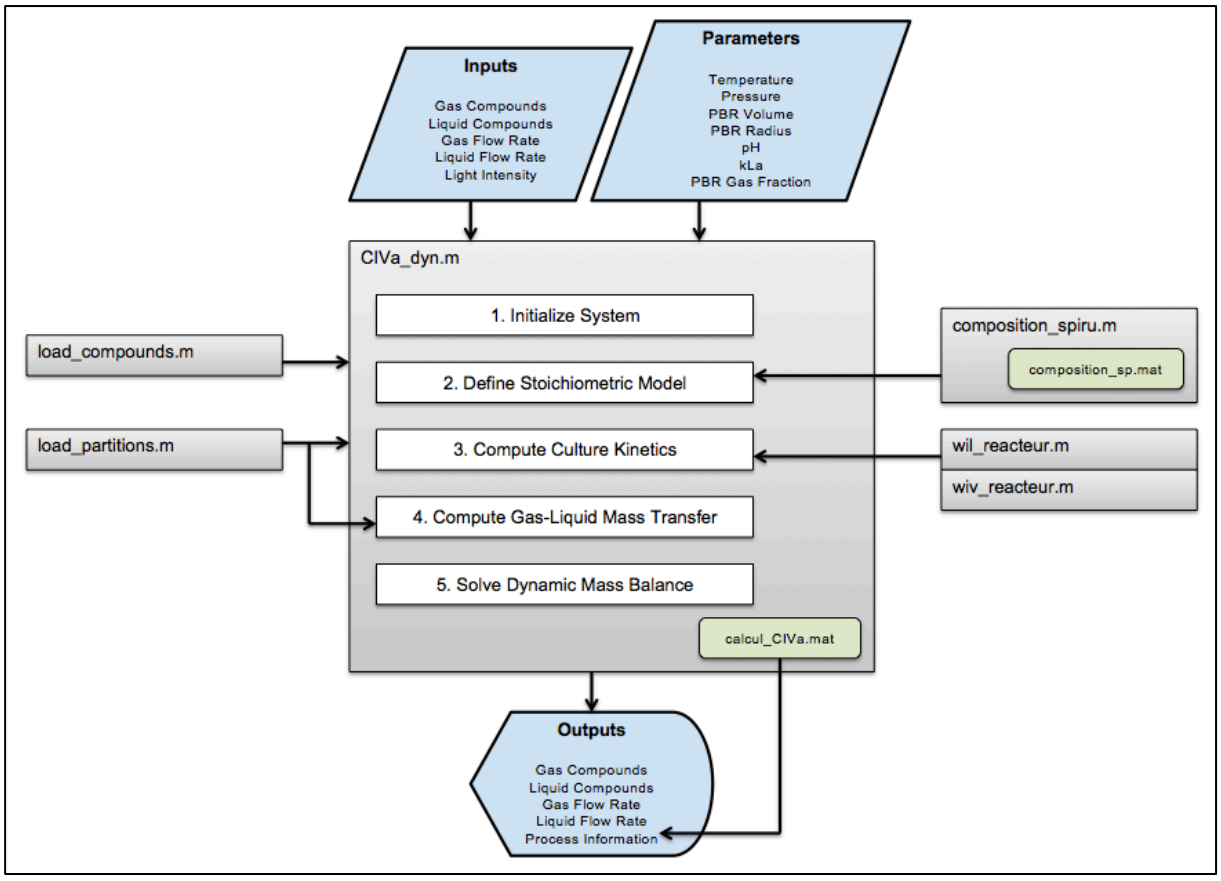

Figure 3.7 Simulink CIVa basic algorithm

3.4. Simulink Control Law

The control law is related to the control of the O_2 level in the crew compartment. The control subsystem initially implemented was a simple control law with two possible light intensity values: maximum (225 $W \cdot m^{-2}$) and minimum (20 $W \cdot m^{-2}$). A switch changed from one value to another, with a given periodicity, depending on if the O_2 current measure was below or above the established setpoint. Although the simplicity of the control law, it succeeded in roughly maintaining the system around the fixed range.

However, to avoid discontinuous changes in the light intensity and to have a more realistic and refined control, an improved O_2 control subsystem was designed. The result is a cascade of controllers adapting smoothly the light intensity to the specific demands (**Figure 3.8**). CV controller calculates the output O_2 for CIVa given the crew O_2 measure and setpoint. On the other hand, CIVa controller calculates the light intensity to be applied.

From the control subsystem point of view, the inputs are the O_2 measures from both compartments, as well as the desired O_2 setpoint for the crew compartment. The output is the light intensity action needed to meet the needs, which serves as an input for the CIVa compartment.

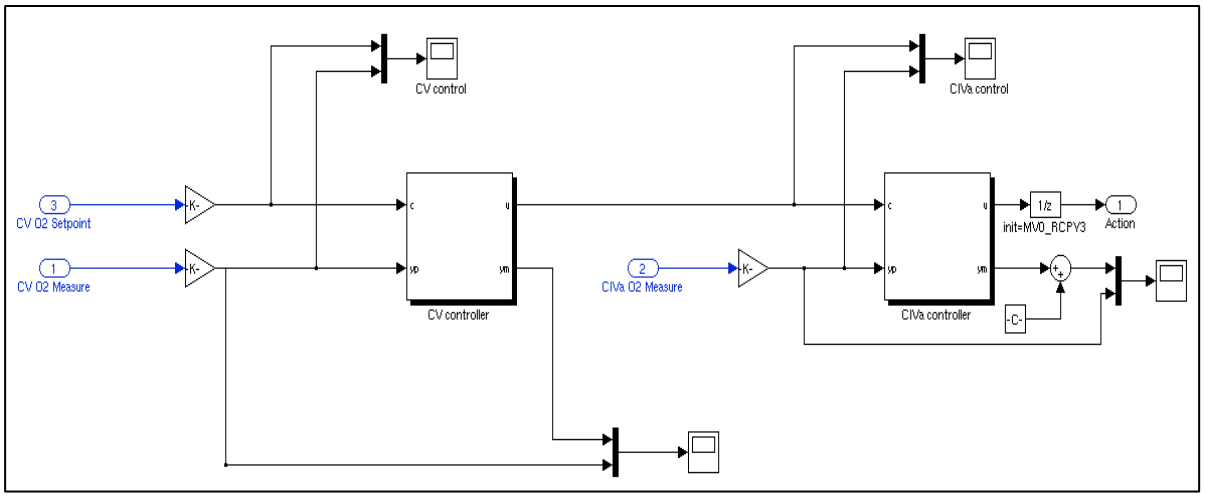

Figure 3.8 Matlab/Simulink control block

The O_2 setpoint can be fixed through the step block called *CV setpoint* and shown in **Figure 3.1** (in red). Within this block, the initial and final O_2 setpoints can be fixed with a specific step time between them, which can especially suitable to simulate dynamic transitions (**Figure 3.9**, left).

Moreover, from the dialog box of the control module (**Figure 3.9**, right), the user can manipulate the light intensity available range, the control period for both compartments and the suitable O_2 range for the photobioreactor compartment.

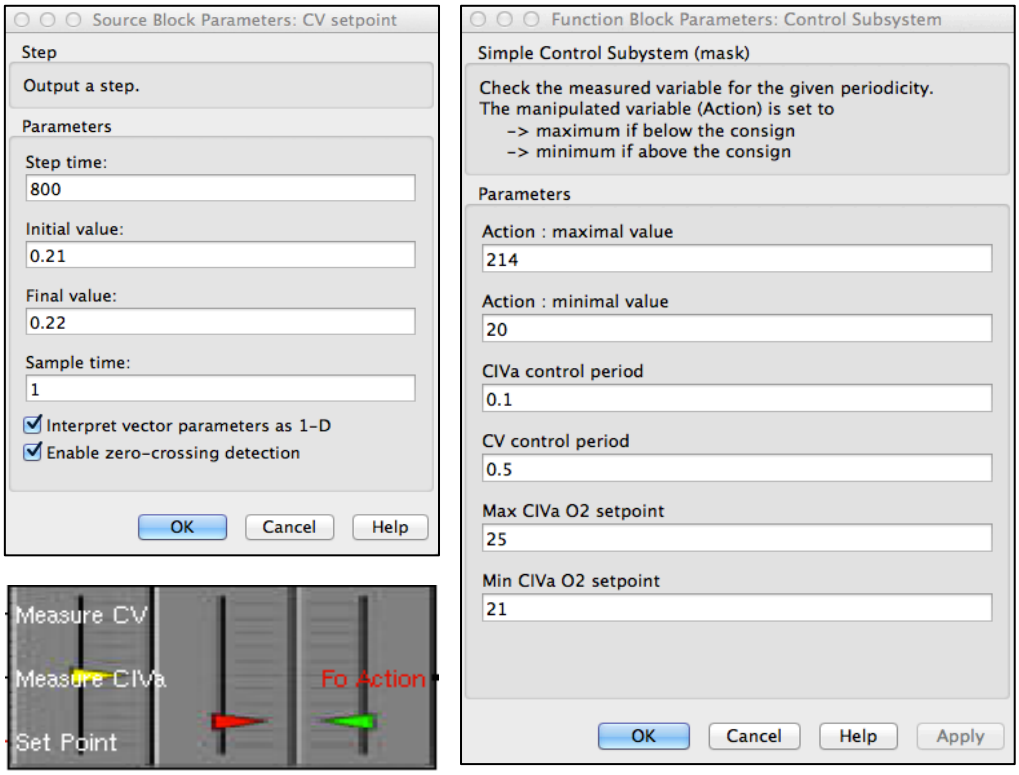

Figure 3.9 Control subsystem main block (bottom left) and dialog boxes (top left and right)

Chapter 4

WP1 RESULTS AND DISCUSSION

4.1. WP1 Experimental Results

The WP1 integration experimental campaign at the MPP started on Tuesday, 26 May 2015, when CV and CIVa were connected with the first group of animals. It successfully finished by Friday, 26 June, making a total of 744 h of operation.

The experimental results here described refer to the first phase of the WP1 integration, where the O_2 level in CV was maintained at 21%. The rest of phases of WP1 (with an O_2 setpoint of 18% and 23%) will be accomplished in the coming months and are not included in this work. The main experimental results obtained in the first phase of WP1 integration are showed below.

The most significant results derived from CV are related to the sustainability of the gas levels (O_2 and CO_2) in the compartment within a specified range to ensure a suitable habitat for the crew. The light intensity provided to CIVa is also significant because it determines, through the control system, the amount of O_2 in the crew compartment and it helps to keep it within the desired setpoint (21% in this case). All these results are shown in **Figure 4.1**.

Sharp peaks displayed in the results are due to some technical problems during the experiment (e.g. power cuts). Fortunately, the system recovered well and the results were not affected by these incidences. However, two days before the end of the experiment (24 June), both compartments were disconnected because there was foam accumulating in the output filters of CIVa. Moreover, The same day, the gas analyser of CV broke down. As a consequence, a big disturbance is shown in the results at around t=700 h, making the last measures not reliable. For this reason, results beyond t=700 h are not taken into account for the analysis.

The first observation from the results in CV is that gas levels increase and decrease in a cyclic way with a period of around 12 hours. This is due to the activity of the crew. Wistar rats follow roughly a 12/12 h day/night cycle, consuming more O_2 at night and less during days. These changes in O_2 demand can be are clearly seen in **Figure 4.1**.

O_2 level is kept around 21% during the whole duration of the experiment. However, there is a tendency of the O_2 to decrease, already evident since t=450 h and more acute between t=600 h and t=700 h. It could be a problem of insufficient O_2 production in the photobioreactor that leads to a progressive decrease of O_2 in the crew compartment, or could also be the consequence of the weight increase of the rats in CV (rats increased their weight up to 10% approximately during the integration test).

In the same way, CO_2 level is maintained below 20000 ppm (2%), fulfilling the objective established. Although CO_2 never surpasses the limit during the test, it gradually accumulates in the crew compartment and this feature could be problematic in longer tests.

Finally, light intensity drives the O_2 level and adapts to the specific needs as can be observed in the results. When O_2 level is below the setpoint, light intensity increases to adjust the demands, while light intensity decreases when O_2 level is above the setpoint. As time passes, light intensity is more time at its maximum capacity trying to recover the O_2 setpoint in CV, as can be shown in the lower graph.

Light intensity was initially limited to 90% of its capacity, equivalent to 203 $W \cdot m^{-2}$ approximately. However, it was observed that O_2 seemed to be slightly decreasing and, as an attempt to increase the level, the light intensity limit was modified to 95% (around 214 $W \cdot m^{-2}$). Even with the change, no significant results are observed, which confirms the previous considerations on the control system.

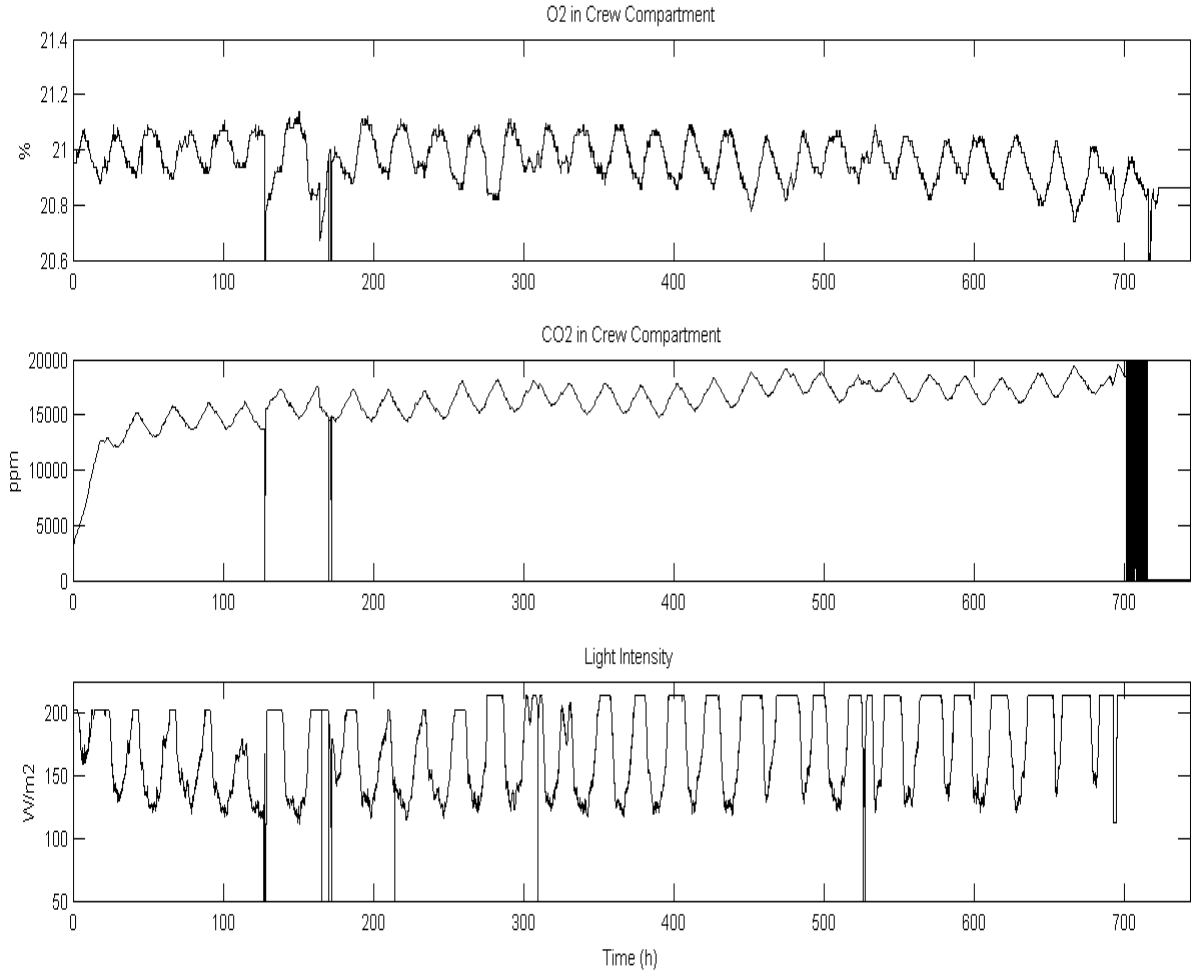

Figure 4.1 O_2, CO_2 and light intensity in Crew Compartment during WP1 first integration

In the case of the photobioreactor, the main results regarding gas levels are shown in **Figure 4.2**.

O_2 level in the photobioreactor is maintained around 21.9% (always more O_2 in PBR to satisfy the crew demands). O_2 levels in CIVa are higher when there is a lack of O_2 in CV (and the other way around), since it is needed to produce more O_2 to satisfy the crew demands.

CO_2 increases gradually like in the crew compartment, although it seems to be finally stabilizing just below 10000 ppm. Due to the gas/liquid transfer, part of CO_2 is transferred to the liquid phase so that there is not a big accumulation of gas CO_2 in the photobioreactor.

It should be highlighted that, even though O_2 and CO_2 levels in CIVa are not directly restricted (as it is the case for CV), it is important to keep the levels inside reasonable margins to allow for a good performance in the crew compartment.

In this case, light intensity is also displayed since it affects directly the *Arthrospira platensis* photosynthesis and therefore the O_2 level in the photobioreactor (O_2 peaks are produced when light is at the maximum capacity). Again, the limitations mentioned before regarding light intensity are taken into account.

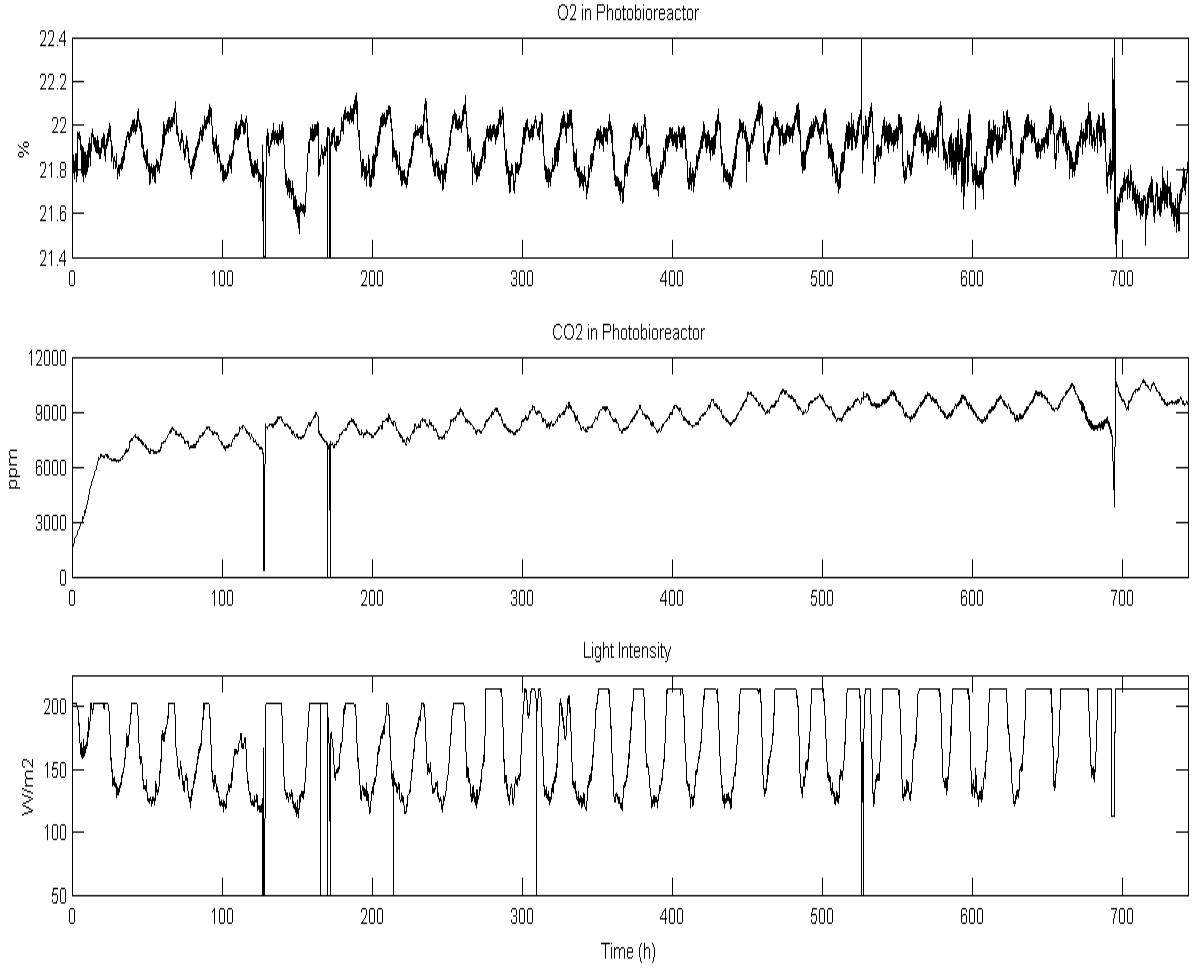

Figure 4.2 O_2, CO_2 and light intensity in Photobioreactor during WP1 first integration

O_2 production by CIVa is also measured within the experiment and it is displayed in **Figure 4.3**. Theses results show the amount of O_2 that needs to be produced to keep the O_2 concentration in CV constant. For this reason, data obtained can be taken roughly as the O_2 consumption in the crew compartment. Results show an oscillatory behaviour with an approximate mean production of 1.5 $g \cdot h^{-1}$ during day and 2.5 $g \cdot h^{-1}$ at nights, which would correspond to the inactive and active periods of the Wistar rats.

It can also be observed from **Figure 4.3** that, during the experiment duration, CIVa appears to be much more time in a high level of O_2 production to compensate the lack of O_2 in the crew compartment. This behaviour may be due to specific changes in the crew activity (e.g. rats spend more time active than inactive) or due to the crew growth.

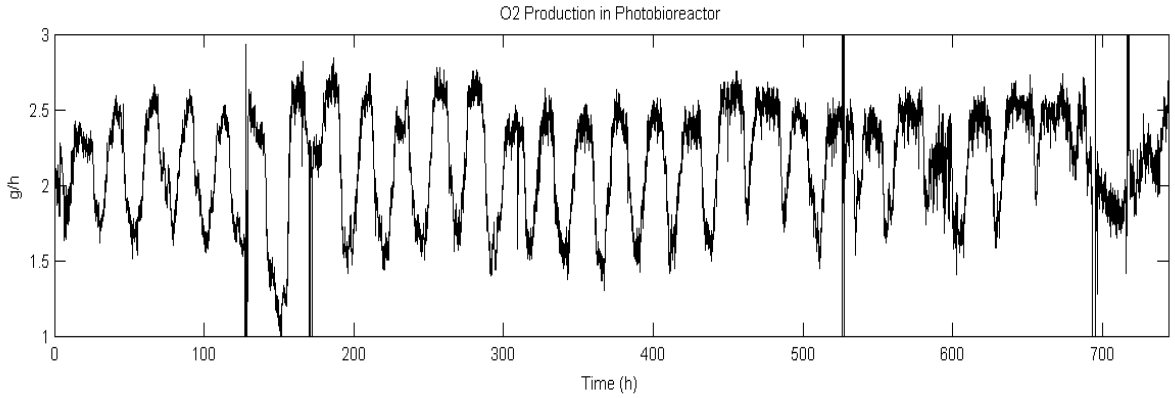

Figure 4.3 O_2 production in Photobioreactor during WP1 first integration

Since WP1 relies on the closure of the gas phase between CV and CIVa, the most significant measures obtained during the experiment are related to the gas compounds involved. However, the biomass concentration of the culture inside the reactor is also measured on-line (liquid phase) to avoid potential problems associated to the lack or excess of biomass (**Figure 4.4**).

From the results displayed, it can be observed that liquid flow rate (F_L) is changed during the experiment. This is done to keep the biomass concentration around 1.2 $g \cdot L^{-1}$ and ensure that way the O_2 production capacity. With the starting flow rate of 0.93 $L \cdot h^{-1}$, biomass decreases and stabilizes at approximately 1.05 $g \cdot L^{-1}$ around t=360 h. Then flow rate is decreased to 0.75 $L \cdot h^{-1}$ to allow an increment in the biomass concentration, until it reaches almost 1.2 $g \cdot L^{-1}$ at t=480 h. Finally, flow rate is increased again to 0.84 $L \cdot h^{-1}$ to try to stabilize the biomass concentration at around 1.2 $g \cdot L^{-1}$.

Related also to the biomass concentration, an anomaly is shown at around 200 h, when biomass increases for a period of time and then decreases again. This phenomenon appears after noise is removed but there is not a clear reason explaining the biomass increment, although it might be due to the malfunctioning of the biomass probe.

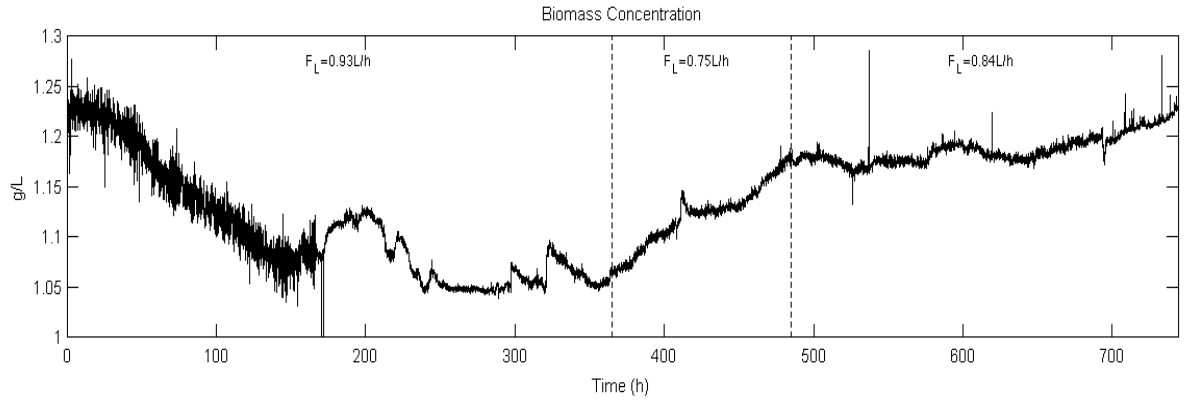

Figure 4.4 Biomass concentration during WP1 first integration with changes in the liquid flow rate

4.2. WP1 Simulation Results

4.2.1. WP1 Simulation Results VS Experimental Results

To simulate the WP1 experiment, the main conditions listed in **Table 4.1** and **4.2** were used. In order to obtain more precise results, data taken directly from the real WP1 integration was considered. In addition to the measures shown before, multiple sensors allowed to obtain data from the WP1 operational conditions and their evolution (e.g. temperature, overpressure, operational volume or pH). Although all these values were found not to be constant, an approximation to a single value was taken for the simulation for the sake of simplicity. An exception is the flow rate, which initially was considered to be constant but in reality was changed for the reasons mentioned in the previous section. Another exception is the operational volume of CIVa, which was slightly altered during the experiment due to the foam problem in the photobioreactor.

The results here enclosed include the comparison between the real and the simulated WP1 experiment.

Table 4.1 Main process parameters of CV used for the simulation

CV MAIN PARAMETERS	NOMINAL VALUE
Volume (L)	1600
Pressure (atm)	1.002
Temperature (ºC)	22
Gas Flow Rate ($L \cdot h^{-1}$)	167.5
Number of rats	3
Rats O_2 Consumption ($g \cdot h^{-1}$)	1.5-2.5
Rats RQ	0.98

Table 4.2 Main process parameters of CIVa used for the simulation

CIVa MAIN PARAMETERS	NOMINAL VALUE
Volume (L)	83*
Pressure (atm)	1.08
Temperature (ºC)	36
Gas Flow Rate ($L \cdot h^{-1}$)	167.5
Liquid Flow Rate ($L \cdot h^{-1}$)	0.93*
Reactor Characteristic Length (m)	0.076
Gas Volume Fraction	0.01
pH	9.5
$k_L a$ (h^{-1})	10.5
Light Intensity ($W \cdot m^{-2}$)	20-214
Arthrospira Initial Concentration ($g \cdot L^{-1}$)	1.23

* Values changed during the simulation

Results obtained through the simulation regarding the crew compartment, as well as those acquired from the real experiment, are shown in **Figure 4.5**.

With respect to the O_2 level in CV, simulated results show, as in the real case, a constant and periodic trend to maintain the 21%. The simulated pattern fits quite well the real data obtained up to t=450 h approximately, when O_2 progressively decreases during the real test. The simulation considers a constant O_2 consumption for the crew (1.5 $g \cdot h^{-1}$ - 2.5 $g \cdot h^{-1}$) and this assumption may not be true for the reasons explained when describing O_2 production in CIVa (**Figure 4.3**). This non-constant O_2 consumption in CV may produce the difference between the experiment and the model results.

CO_2 behaviour in the simulated model is quite different from the test. Real data show levels of CO_2 between 15000 and 19000 ppm, whereas in the simulation CO_2 stabilizes just below 10000 ppm. This significant difference may come from the gas/liquid transfer model of CO_2 in the photobioreactor, ruled mainly by its coefficient partition. $k_{CO_2}^{ap}$ was calculated in Chapter 2 considering all CO_2 ionic forms were in equilibrium whatever the dynamics of CO_2, but maybe this is not the case. The discrepancies between reality and model show that the determination of $k_{CO_2}^{ap}$ may need to be further investigated.

Light intensity differences between the model and the experiment are not very significant. Cycles are followed fairly well, with major differences encountered during low light intensity periods. These differences may be explained by different factors, one of them being the high sensitivity of the illumination system with respect to the O_2 consumed by the crew (analyzed in the following section).

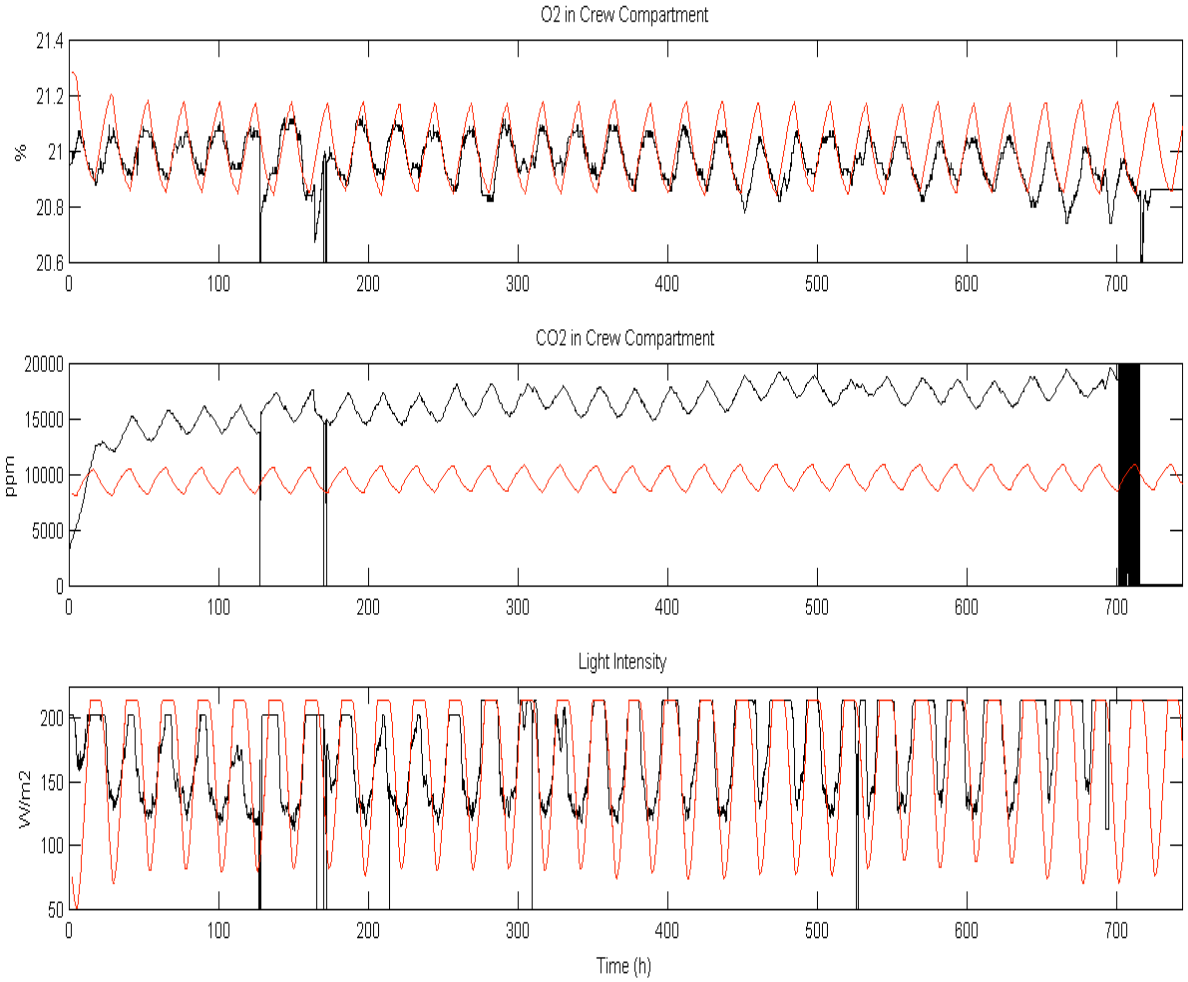

Figure 4.5 O_2, CO_2 and light intensity in Crew Compartment for WP1 experiment (black) and model (red)

The evolution of O_2 and CO_2 in the photobioreactor is very similar to the crew compartment and the results obtained are displayed in **Figure 4.6**.

O_2 level in the simulation show a small delay of the peak measures, although the differences between the real test and the model are minimal. Measures show in both cases O_2 levels between 21.8% and 22% approximately.

From the measure of CO_2 level in CIVa, the same conclusion as in CV can be extracted and gas/liquid dynamics may be more complex than what is modelled. Simulated CO_2, instead of accumulating in the gas phase as in the real case, is also affected by the transfer to the liquid phase. This leads to CO_2 concentrations of around 800 ppm at the end of the simulation, thus impacting in the CO_2 level found in the crew compartment.

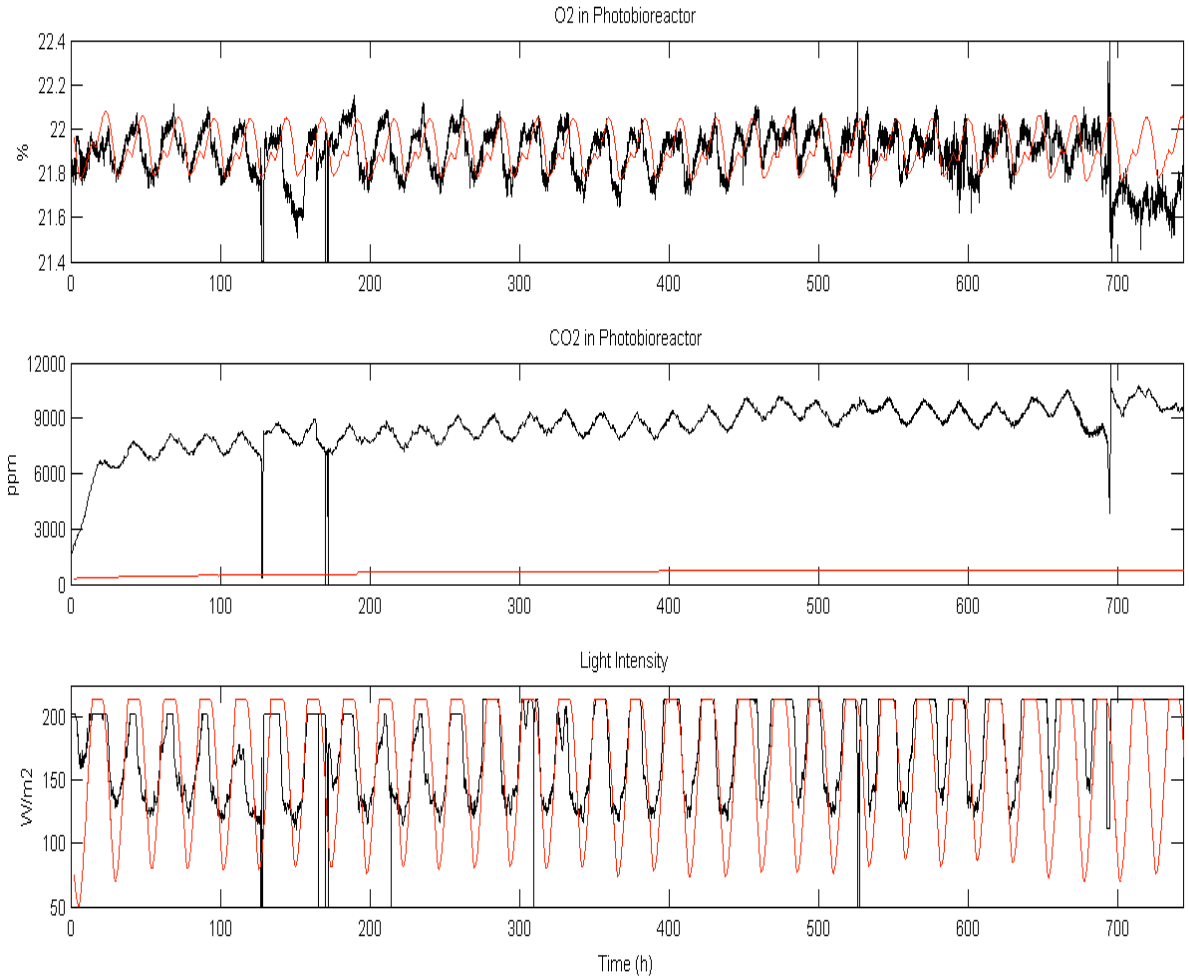

Figure 4.6 O_2, CO_2 and light intensity in Photobioreactor for WP1 experiment (black) and model (red)

Finally, biomass concentration comparison is shown in **Figure 4.7**. With the starting liquid flow rate of 0.93 $L \cdot h^{-1}$, the biomass in the experiment tends to stabilize at a lower level than the one predicted by the model (around 1.08 $g \cdot L^{-1}$ in the simulation and 1.05 $g \cdot L^{-1}$ in reality). When flow rate is decreased to 0.75 $L \cdot h^{-1}$, comparisons are difficult to make since the steady state is never reached. From experimental results, there is a stabilization of the biomass for more than a day at around t=420 h, leading to a delay with respect to the model and therefore an increment in the divergence between experiment and model (around 1.25 $g \cdot L^{-1}$ in the simulation and 1.18 $g \cdot L^{-1}$ in reality). Finally, when flow rate is changed to 0.84 $L \cdot h^{-1}$, biomass seems to stabilize around 1.2 $g \cdot L^{-1}$ in both cases, even though longer tests should be made to confirm it.

Main differences between the experiment and the model (if the delay is not taken into consideration) are probably due the light intensity. Moreover, other possible reasons explaining this feature may be related to the hydrodynamics of the system (model assumes a perfectly mixed reactor and maybe it is not the case) or the growth rate dynamics (maybe there is CO_2 limitation in the photobioreactor).

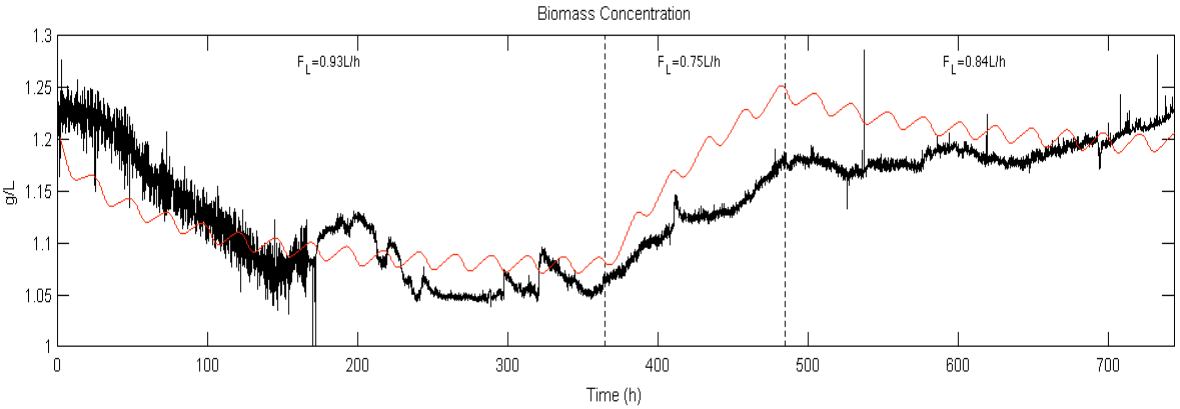

Figure 4.7 Biomass concentration for WP1 experiment (black) and model (red) with changes in the liquid flow rate

4.2.2. Evaluation of the Model

The performance of the model used for the WP1 integration can be considered quite positive in general taking into account that model and experimental data coincide with a 10% margin of error. However, it seems clear that some improvements need to be done in the model to obtain more accurate results. Some of the potential improvement areas are listed below:

- Metabolic model for the crew

The metabolism of Wistar rats is very difficult to model, with an unpredictable behaviour most of times. Aspects like the temperature, the humidity, the diet, the crew growth or specific stress situations (e.g. external noise) may affect the behaviour of the crew and are not taken into account in the model because of its complexity and randomness. At the same time, the 12/12 h cycle modelled is only a general approximation and the reality may differ considerably.

The main parameter used to define the metabolism of rats is the respiration rate, understood as the O_2 consumption rate. As mentioned in previous sections, O_2 consumption for WP1 is assumed to be around 1.5 $g \cdot h^{-1}$ during days and 2.5 $g \cdot h^{-1}$ at nights. This consideration impacts on the light intensity and hence biomass concentration as shown in **Figure 4.8**.

Figure 4.9, on the other hand, displays the same results if O_2 consumption is slightly modified to 1.6 $g \cdot h^{-1}$ – 2.5 $g \cdot h^{-1}$, which could be also taken as a valid assumption for the WP1 model.

Despite the small change between both respiratory behaviours, results show significant differences. Increasing the O_2 consumption during the day implies a growth in the crew demand, which leads to an increment in the needed light and thus an increment in the biomass concentration (more light translates into more biomass production).

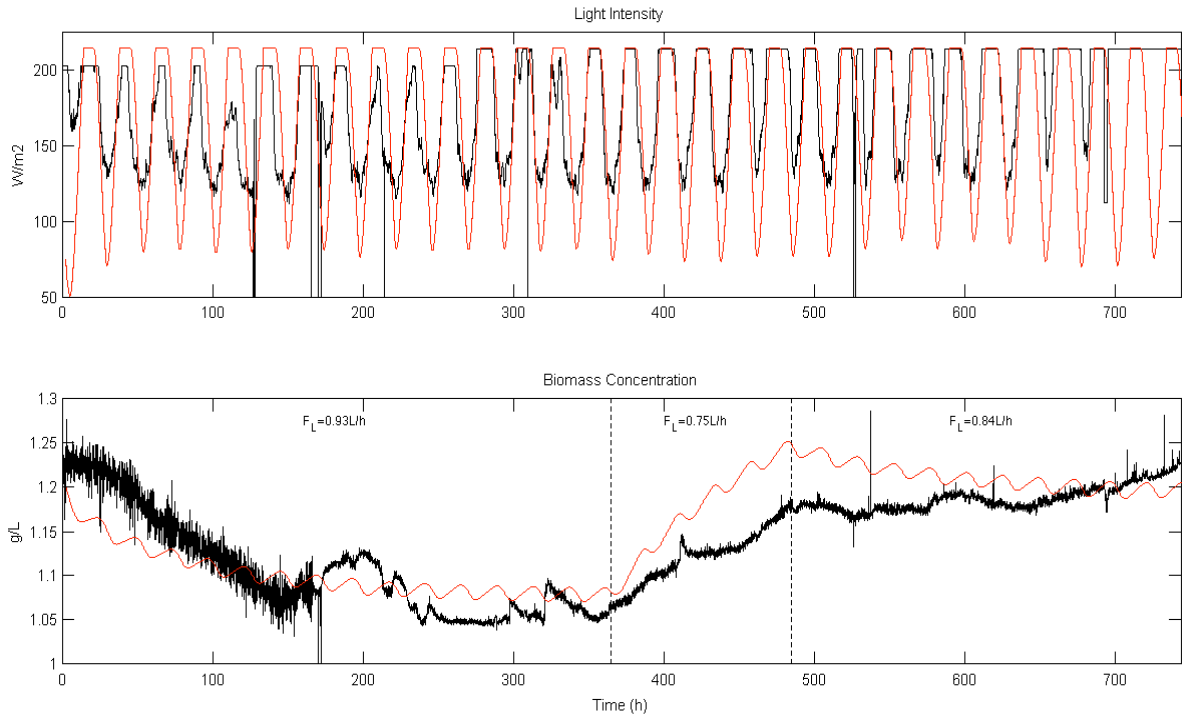

Figure 4.8 Light intensity and biomass concentration for WP1 experiment (black) and model (red) with a mean O_2 consumption of 1.5 $g \cdot h^{-1}$ – 2.5 $g \cdot h^{-1}$

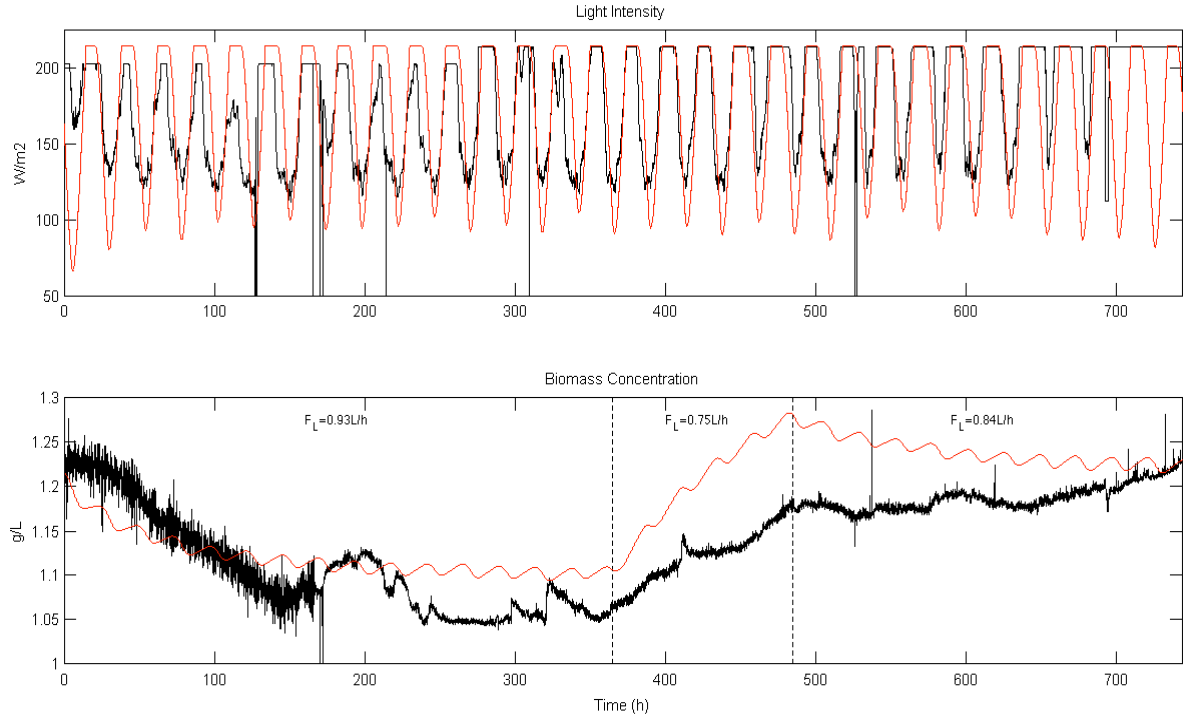

Figure 4.9 Light intensity and biomass concentration for WP1 experiment (black) and model (red) with a mean O_2 consumption of 1.6 $g \cdot h^{-1}$ – 2.5 $g \cdot h^{-1}$

- Dynamics of CO_2 mass transfer

As mentioned before, CO_2 issue in both compartments may be due to CO_2 transfer between the gas and liquid phase. The $k_{CO_2}^{ap}$ model followed needs a revision since real data show that CO_2 transfer and bicarbonate consumption may be a possible limitation. To evaluate the relevance of the CO_2 dynamics in the system, the model is run for different k_{CO_2} values.

If ionic forms are not considered, k_{CO_2} is roughly 2000 in MPP conditions, meaning that the molar fraction of CO_2 at equilibrium is 2000 times higher in the gas phase than in the liquid phase. Results for this hypothesis (**Figure 4.10**) show an imbalance in CO_2 accumulation in both compartments. Most CO_2 remains in the gas phase and accumulates and from a realistic point of view this scenario does not make sense.

On the other hand, when ionic forms are considered, current model relying on pH shows a k_{CO_2} value around 1.5 (approximately the same CO_2 molar fraction in the gas and liquid phase at equilibrium). In this case, results displayed in **Figure 4.11** are the same as those obtained in 4.2.1 and evidence probably a too optimistic approach regarding CO_2 accumulation in the gas phase. Following this model, **Figure 4.12** shows the CO_2 performance if a k_{CO_2} of the order of 20 is considered. Results obtained are quite accurate, especially for the crew compartment, and demonstrates that CO_2 behaviour in the system is very sensitive to k_{CO_2} and for that reason a more accurate model should be developed.

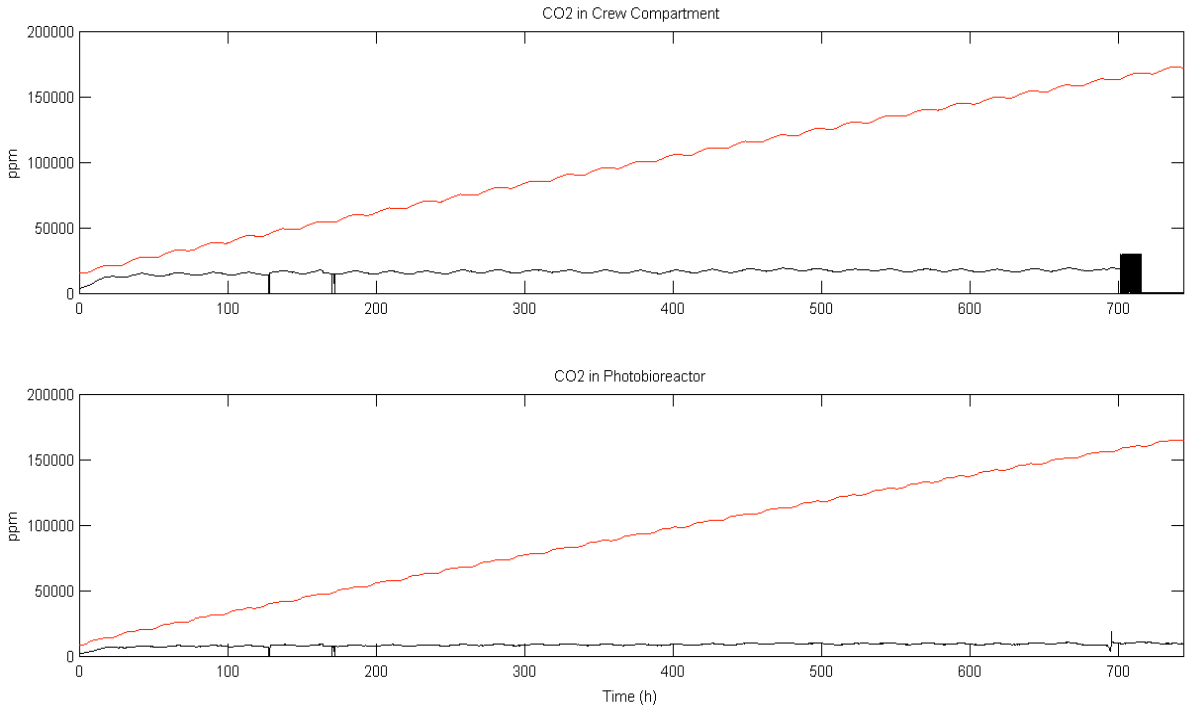

Figure 4.10 CO_2 in Crew Compartment and Photobioreactor for WP1 experiment (black) and model (red) with k_{CO_2} = 2135

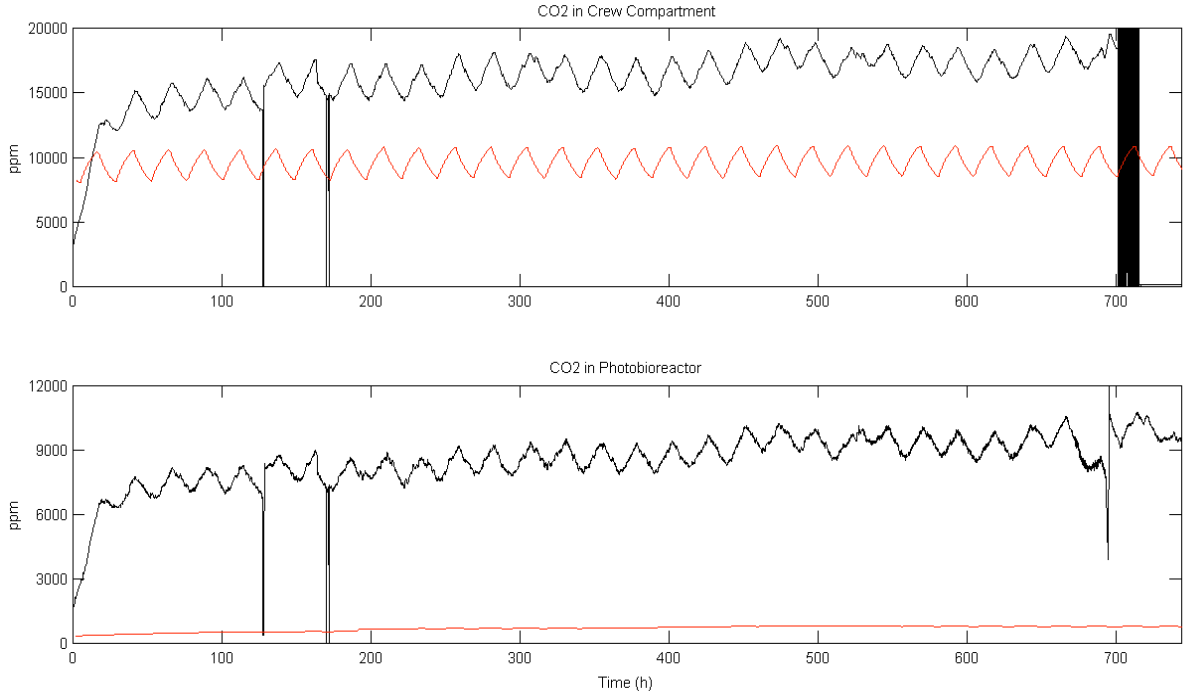

Figure 4.11 CO_2 in Crew Compartment and Photobioreactor for WP1 experiment (black) and model (red) with k_{CO_2} = 1.63

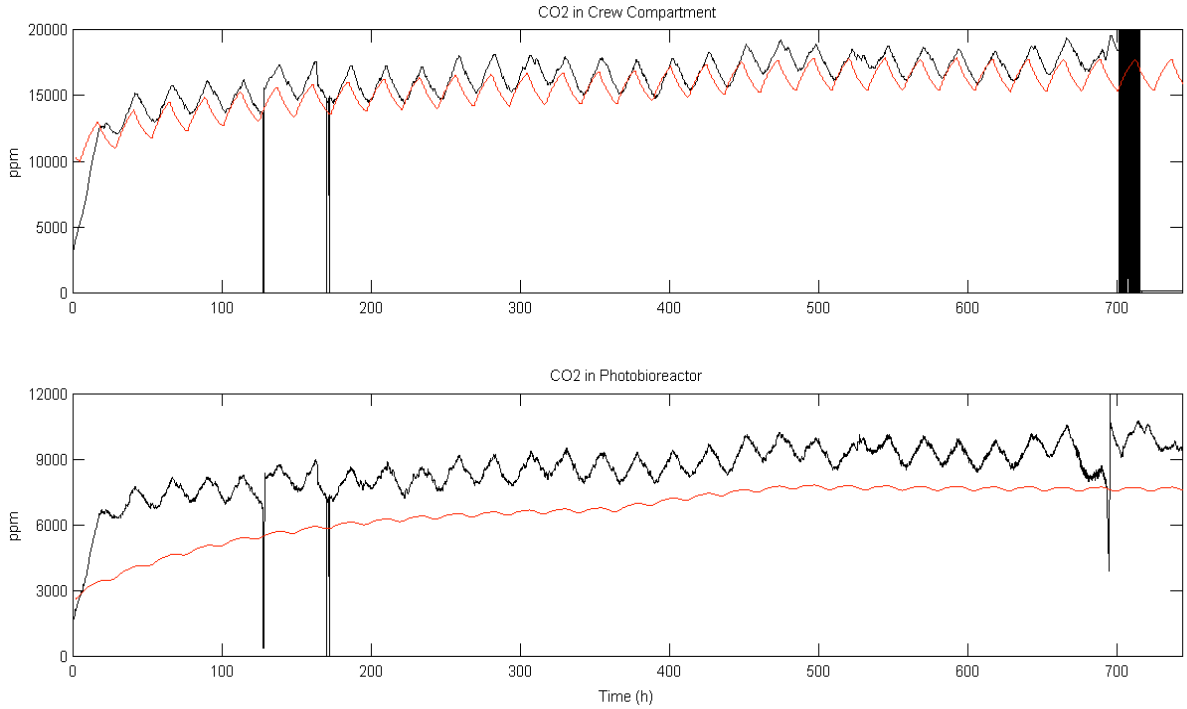

Figure 4.12 CO_2 in Crew Compartment and Photobioreactor for WP1 experiment (black) and model (red) with k_{CO_2} = 20

- Photobioreactor productivity

The light model used within the simulation and developed by J.F. Cornet relies on the knowledge of the maximum specific growth rate (μ_{max}) of the culture. However, current research about productivities in photobioreactors shows an improved light model based thermo-kinetic coupling laws. This new type of model, also developed by J.F. Cornet [23] presents a higher degree of knowledge if compared to the previous one. Therefore, the performance of the model may be increased if the light model is updated.

- Non-constant conditions in CV and CIVa

The model assumes that most conditions inside compartments are constant during the whole simulation (e.g. overpressure, volume, temperature, flow rate or pH). However, data obtained from the integration test demonstrate that this is not entirely true (not taking into account discontinuous variations due to changes in the operational conditions). **Figure 4.13** shows real measures of those conditions and the values implemented in the model. Probably results are still quite acceptable, but to obtain an even more realistic model maybe all these variations should be considered.

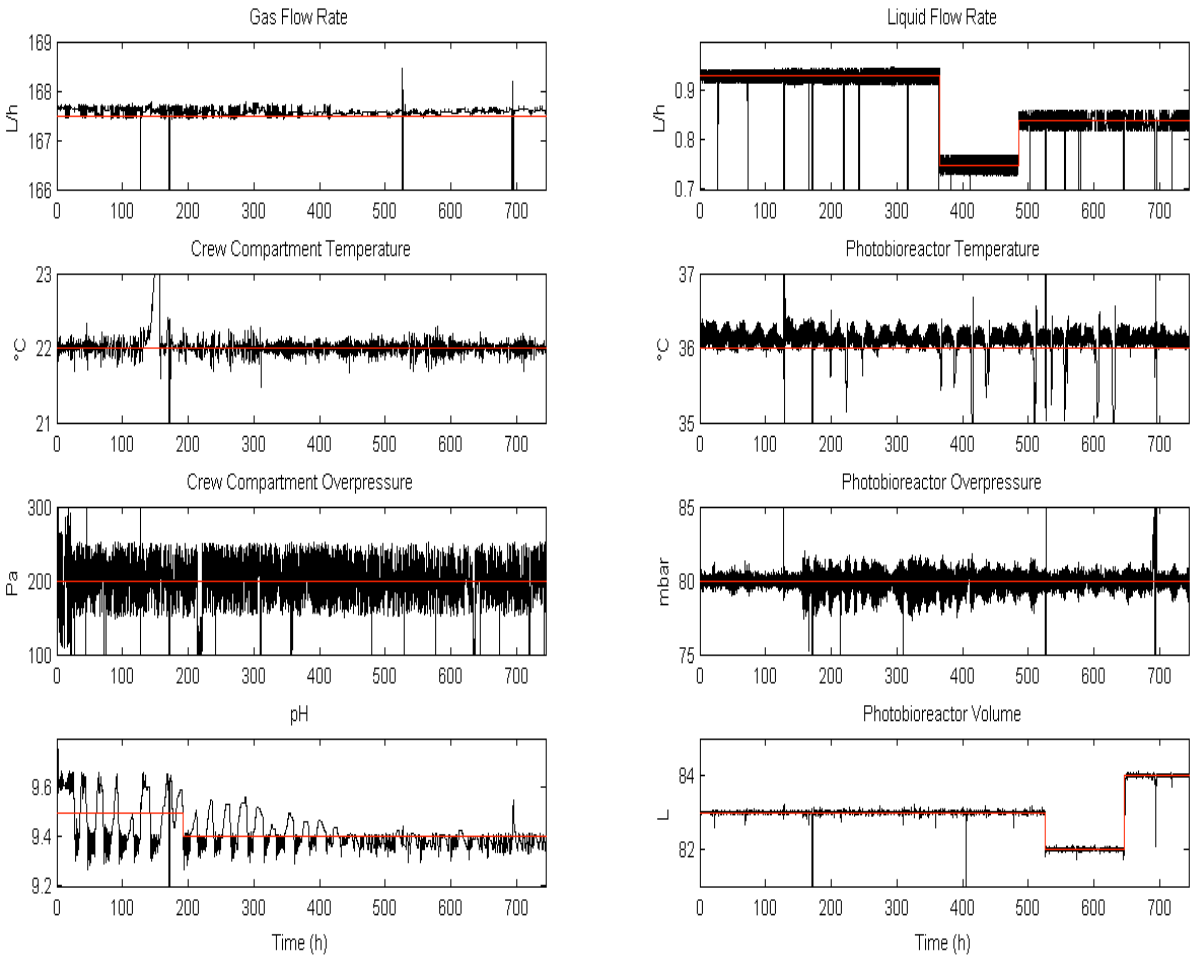

Figure 4.13 Main parameters for WP1 experiment (black) and model (red)

4.3. WP1 Model Exploitation

Taking into account that the objective of this work has already been achieved, since WP1 model has been analysed and compared with experimental data, a further step can be considered.

The simulation tool offers countless possibilities, giving the opportunity of evaluating other operational conditions and/or unexpected potential perturbations in the operation of the system. Therefore, this final section of the work takes into account the exploitation of the WP1 model, using nominally the parameters already described in **Table 4.1** and **4.2** (not considering changes during the simulation) with a liquid flow rate of 0.84 $L \cdot h^{-1}$.

The model exploitation can be divided into two different sections: the simulation of the remaining WP1 integration phases and the simulation of different kind of perturbations.

4.3.1. WP1 Remaining Phases

With the final objective of extending the WP1 simulation to the other phases involved (18% and 23% O_2 in CV), the dynamic and steady state responses of the system in both cases have been simulated.

Even though steady state is simulated, the main objective of this section is to analyse the dynamic response during the transition between O_2 setpoints (21% to 18% and 21% to 23%) in WP1 nominal conditions. For this reason, the stabilization time is the most significant parameter to examine.

- From 21% to 18%

The second WP1 integration phase sets the O_2 level to 18%. **Figure 4.14** shows the results of a test starting at 21% O_2 in the crew compartment and ending at 18%, paying special attention when the system moves from one setpoint to the other.

The change of setpoint is produced at t=100 h. At this moment, light is set at its minimum intensity (20 $W \cdot m^{-2}$) to reduce the O_2 level. During this period of low light intensity, biomass concentration drops to 0.8 $g \cdot L^{-1}$ and O_2 in the photobioreactor also decreases while CO_2 increases in both compartments (surpassing 1000 ppm in CIVa).

At t=160 h, O_2 level reaches 18% and light intensity increases in order to stabilize the O_2 around the current setpoint. However, the system is not fully stabilized until t=230 h approximately, when O_2 is finally maintained at the setpoint and the light intensity cycle is restored. As a result of this process, CO_2 levels in CIVa and CV decrease and stabilize and biomass concentration returns to a level of 1.2 $g \cdot L^{-1}$.

System is able to withstand fairly well the transition between 21% and 18% and the stabilization time could be set at 130 h or 5.5 days, although this time could be

reduced if the illumination system were switched off instead of working at the minimum level.

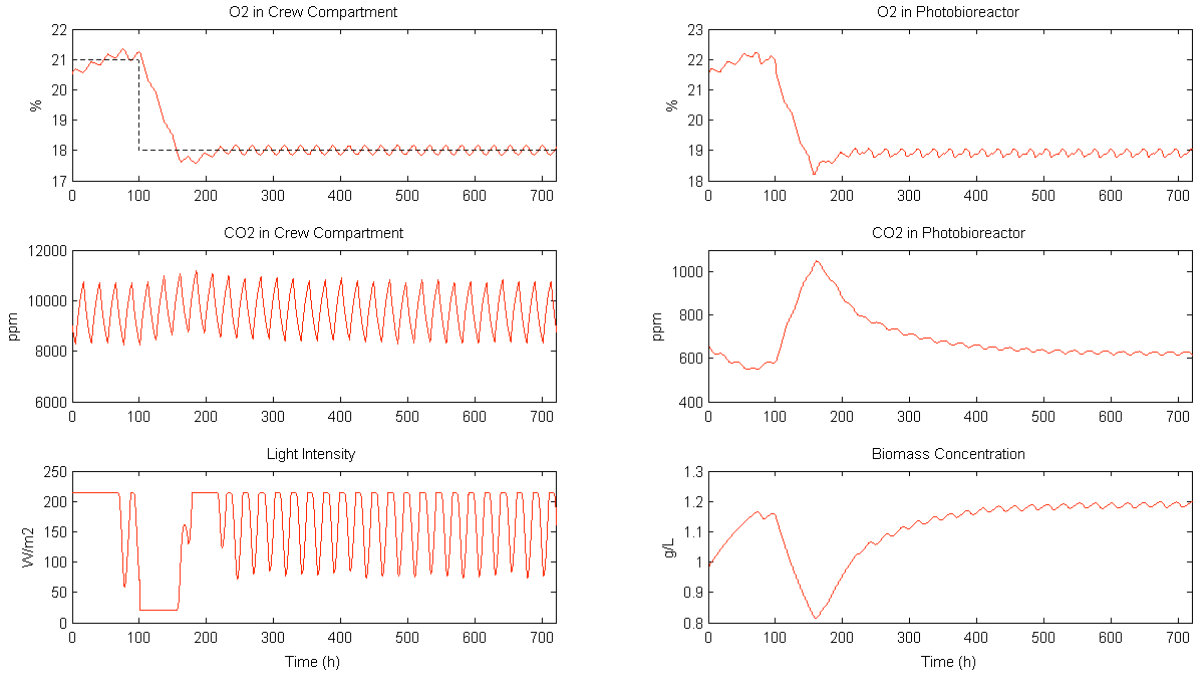

Figure 4.14 Main results for WP1 test with transition from 21% to 18% O_2 in CV

- From 21% to 23%

The third and last WP1 integration phase relies on an O_2 level of 23% and the resulting data from the simulation are displayed in **Figure 4.15** as in the case before.

The transition from 21% to 23% starts again at t=100 h. To increase the O_2 level in the crew compartment, light intensity works at the maximum capacity (214 $W \cdot m^{-2}$) for around 200 h. As a side effect, CO_2 concentration in both compartments slightly decreases and biomass increases up to 1.33 $g \cdot L^{-1}$.

O_2 level reaches 23% shortly before t=300 h but it is not stabilized until approximately 60 hours later, at t=360 h. By that time, light intensity recovers its initial cycle and biomass concentration decreases and returns again to its nominal value of 1.2 $g \cdot L^{-1}$. On the other hand, CO_2 levels tend to increase before they also become stable.

In this case of transition between 21% and 23%, the stabilization time is of the order of 260 h (almost 11 days), a higher time compared with the transition between 21% and 18%. At 21%, the illumination system is used to working at relatively high light intensity levels. For that reason, changing to a higher setpoint is far less “effective” because the overall change in light intensity is lower and thus it translates into a higher stabilization time.

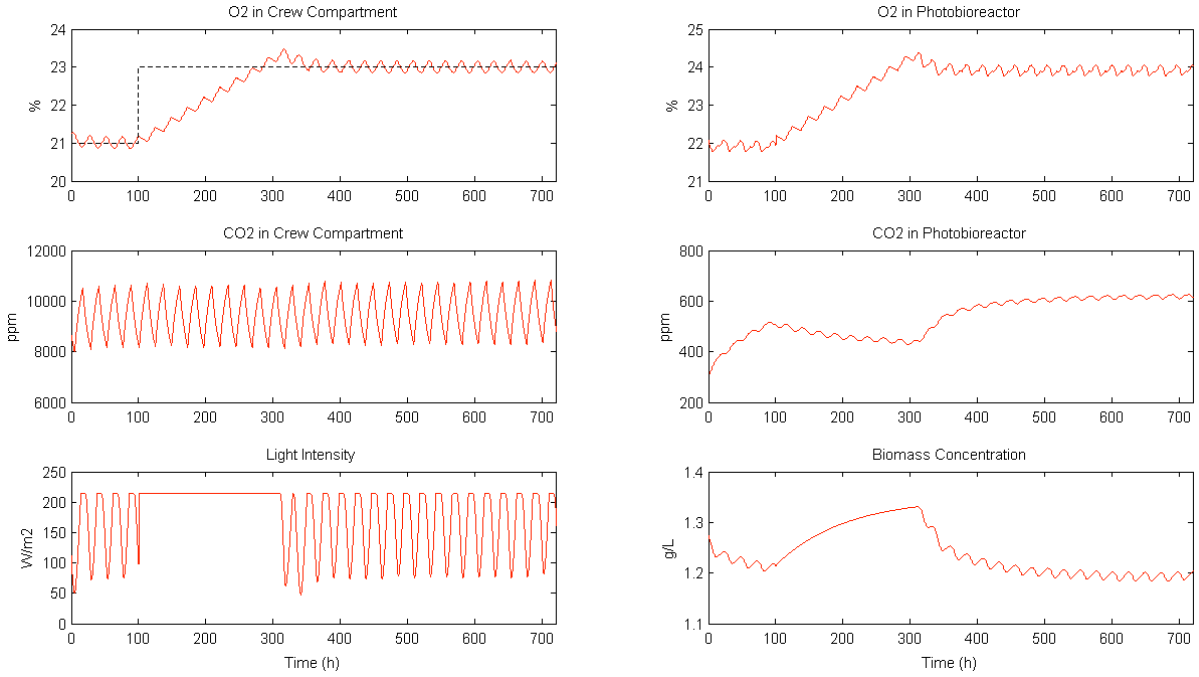

Figure 4.15 Main results for WP1 test with transition from 21% to 23% O_2 in CV

4.3.2. Perturbations

With the additional purpose of gaining more knowledge about potential realistic scenarios, some perturbations can be added to the system to see how it reacts to them. This is the aim of this section, to use the simulation tool to analyse how the system behaves in different potential scenarios and to foresee possible limitations in the system without the need to carry out additional experiments.

It is remarkable to realise that perturbations can be linked to a lot of parameters within the system and to get more realistic data the simulation model would need to be changed to adapt better to the real behaviour (i.e. to simulate mineral limitations, the growth kinetics of the culture has to be entirely modified, since the current model only takes into account light limiting conditions). With these considerations, the perturbations analysed in this section are based on a level of 21% O_2 in CV and are divided according to the compartment associated.

Associated to the crew compartment, two perturbations are considered regarding the crew itself: a change in the number of rats and a change in their activity.

- Change number of rats

The model is used here to verify the hypothesis of using 4 rats for the WP1 integration and see how the system behaves. In addition, WP1 integration with 2 rats is also simulated.

Figure 4.16 shows the results of WP1 when 4 rats are take into account. Data obtained demonstrate that 4 rats cannot be used for the WP1 and that is exactly what happens in reality.

From the very beginning, light intensity is set at maximum and remains there for the whole duration of the test, forcing the production of O_2 in the photobiorecator to meet the increased demands of the crew. However, CIVa, even at the maximum capacity of production, is not able to produce enough O_2 and O_2 level in CV starts to decrease progressively (leading to a decrease also in CIVa). The effects of the illumination system can also be noticed in the biomass concentration, increased and stabilized up to 1.35 $g \cdot L^{-1}$. CO_2 accumulation is not a problem in this case, although it cannot be ensured due to the fact that current model regarding CO_2 dynamics needs a revision.

The time of reaction in this case could be set at around t=240 h (10 days), when O_2 in the crew compartment reaches a limit level of 17%. Below this value, consequences for the crew may be dramatic.

Furthermore, results using 2 rats are displayed in **Figure 4.17**. Since WP1 works with 3 rats, it will also work with 2, since the demands of the crew are lower. Even though, it is interesting to appreciate how the system performs with less demanding conditions.

From the results obtained, low values of light intensity (around 50% of its capacity at worst) are needed to maintain O_2 levels in both compartments within the desired range. Due to the lower light intensity, biomass concentration decreases to 0.8 $g \cdot L^{-1}$. Finally, less demands in the crew compartment translates to less CO_2 accumulation in both compartments if compared with the case of a crew formed by 3 rats.

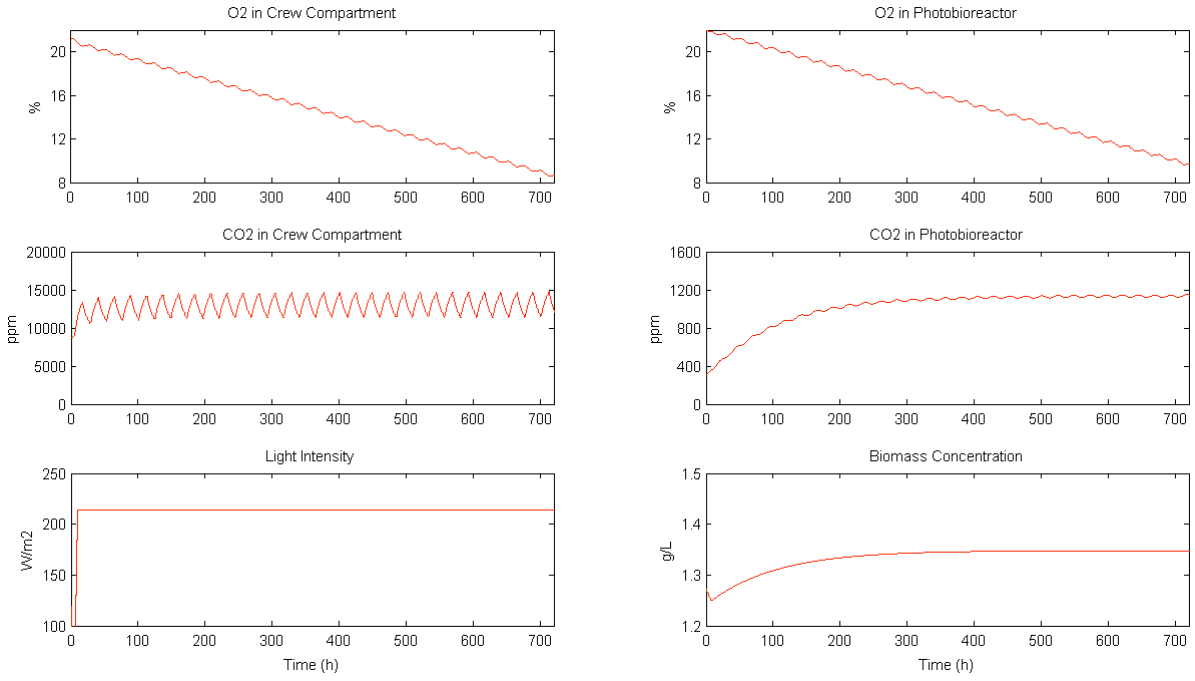

Figure 4.16 Main results for WP1 test with 4 rats

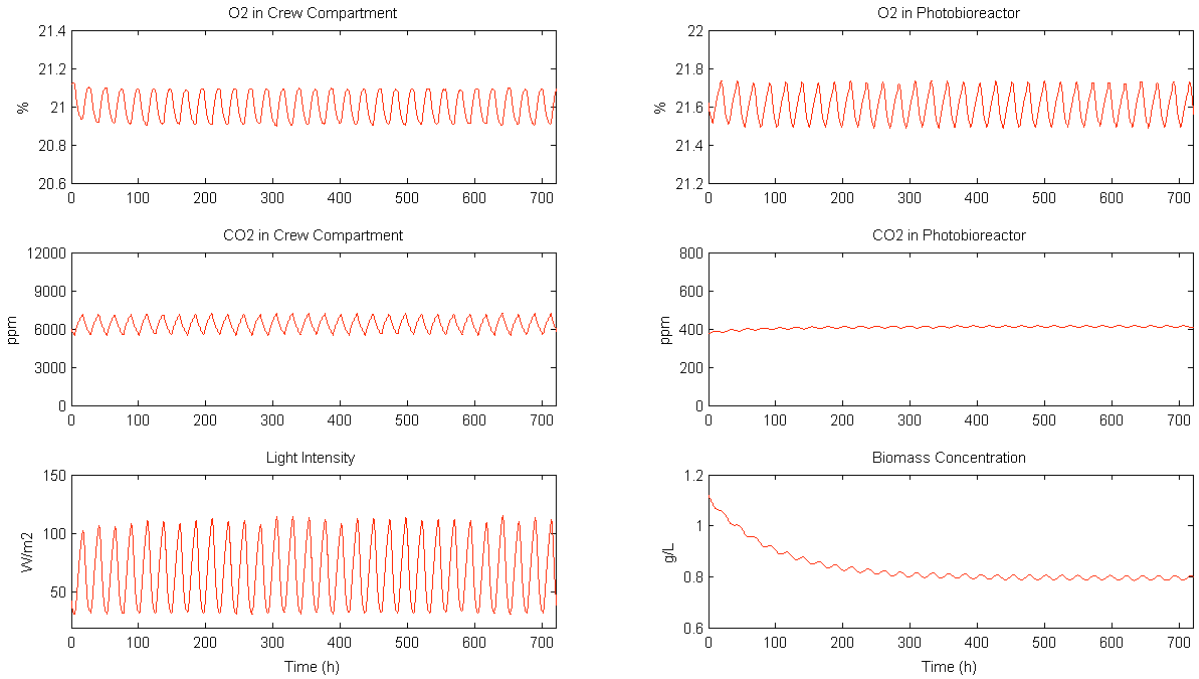

Figure 4.17 Main results for WP1 test with 2 rats

- Change in rats activity

For the purpose of the WP1 integration, a 12/12 h cycle (night and day) is considered, meaning that rats are 12 h asleep at nights (active) and 12 h awake during days (inactive) respectively. This section simulates what happens to the system if the crew is induced to a cycle of 10/14 h and 14/10 h.

For the 10/14 h cycle, results are shown in **Figure 4.18**, whereas **Figure 4.19** shows the results for the 14/10h cycle. At first sight, differences between the two hypothesises are not very significant and the system is able to withstand both cycles without any problem.

With a 10/14 h cycle, rats are assumed to spend 10 hours/day with a high level of O_2 consumption (night) and 14 hours/day with a low level (day). As a result, O_2 demand in CV is in average lower with respect to the 12/12 h cycle and thus the illumination system is less time in a high level of intensity. As a side effect, biomass concentration stabilizes at roughly 1.15 $g \cdot L^{-1}$ instead of 1.2 $g \cdot L^{-1}$, which would be hypothetically the case if the 12/12 h cycle were considered.

On the other hand, with a 14/10 h cycle, rats spend more time a day active (if compared with the 12/12 and 10/14 cycles) and therefore the average O_2 demand is higher. This translates into an increase in the time at high light intensity level and thus an increase in the biomass concentration (around 1.24 $g \cdot L^{-1}$ at the end of the simulation).

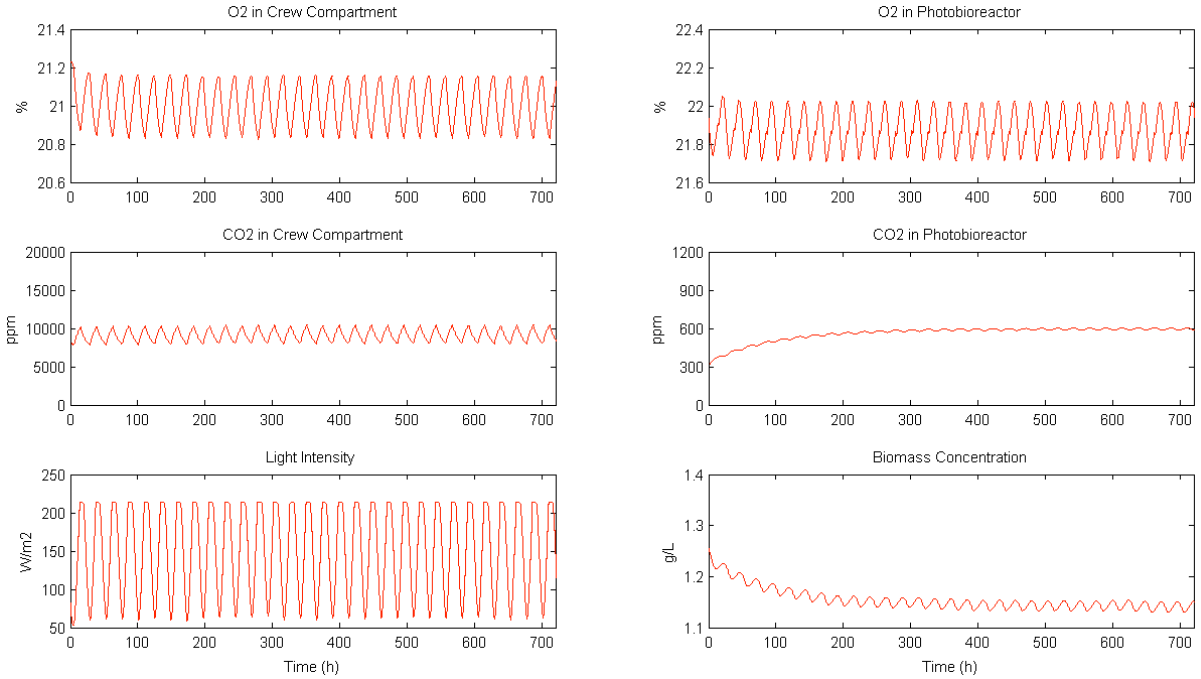

Figure 4.18 Main results for WP1 test with a 10/14 h cycle

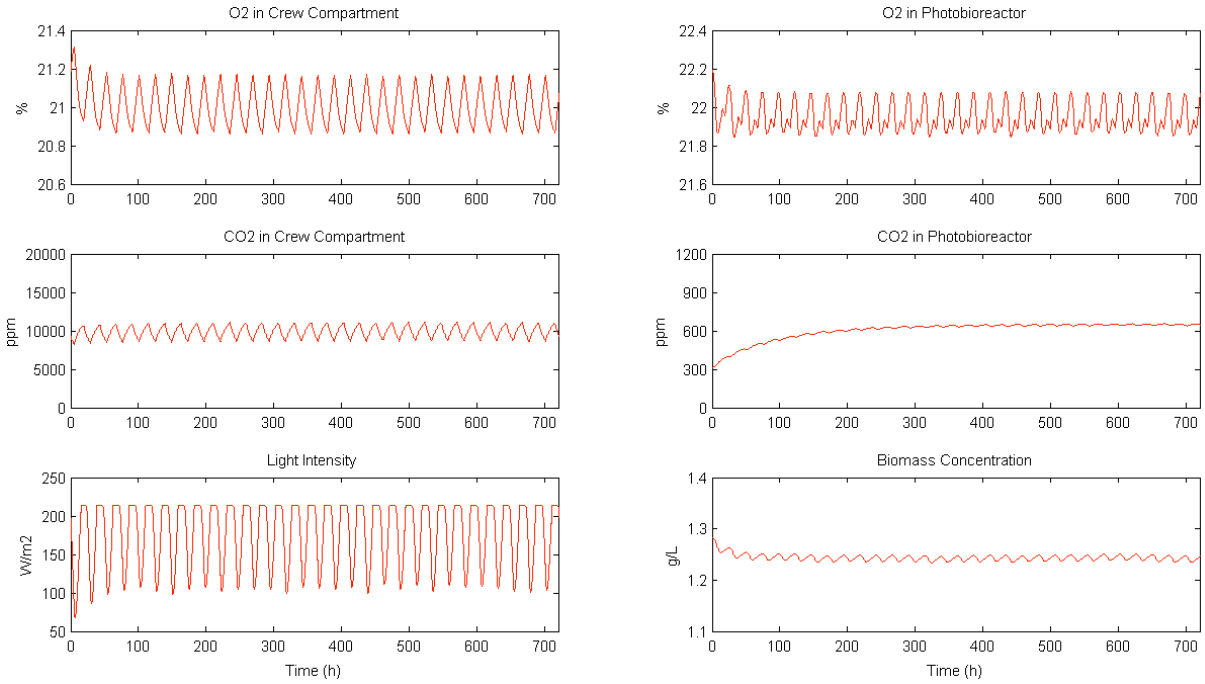

Figure 4.19 Main results for WP1 test with a 14/10 h cycle

Finally, the perturbations associated to the photobioreactor compartment considered are the following: a sudden interruption of the illumination system, a continuous operation with maximum illumination, a change in the $k_L a$ and a change in the *Arthrospira platensis* stoichiometry.

- Interruption of the illumination

One of the critical undesired perturbations that may arise during the WP1 integration is the interruption of the illumination system (e.g. because of a power cut). At the moment the lights were switched off, system would inevitably and progressively decrease its performance. Therefore, the aim of simulating this perturbation is to have an approximate idea of the time lapse before consequences of the perturbation become irreversible.

Data obtained from the simulation are shown in **Figure 4.20** and considers the hypothesis of a shut down of the illumination system at t=100 h. The main consequence of a lack of light in the photobioreactor is clear: the culture stops generating O_2 (O_2 decreases in CIVa) and as a result the crew demands are not satisfied and O_2 also decreases in the crew compartment, reaching a 0% level around t=350 h, 250 hours (a bit more than 10 days) after the illumination system is interrupted. At the same time, biomass concentration drops to almost 0 $g \cdot L^{-1}$ at t=350 h and CO_2 accumulates in CV and CIVa, with levels of around 12000 ppm in the crew compartment and 2000 ppm in the photobioreactor at the end of the simulation.

The critical point to determine the time lapse in this case is set when O_2 level in CV reaches a 17% (see section 2.1.1). Therefore, the reaction time after the interruption of the illumination system would be of 50 hours or 2 days approximately.

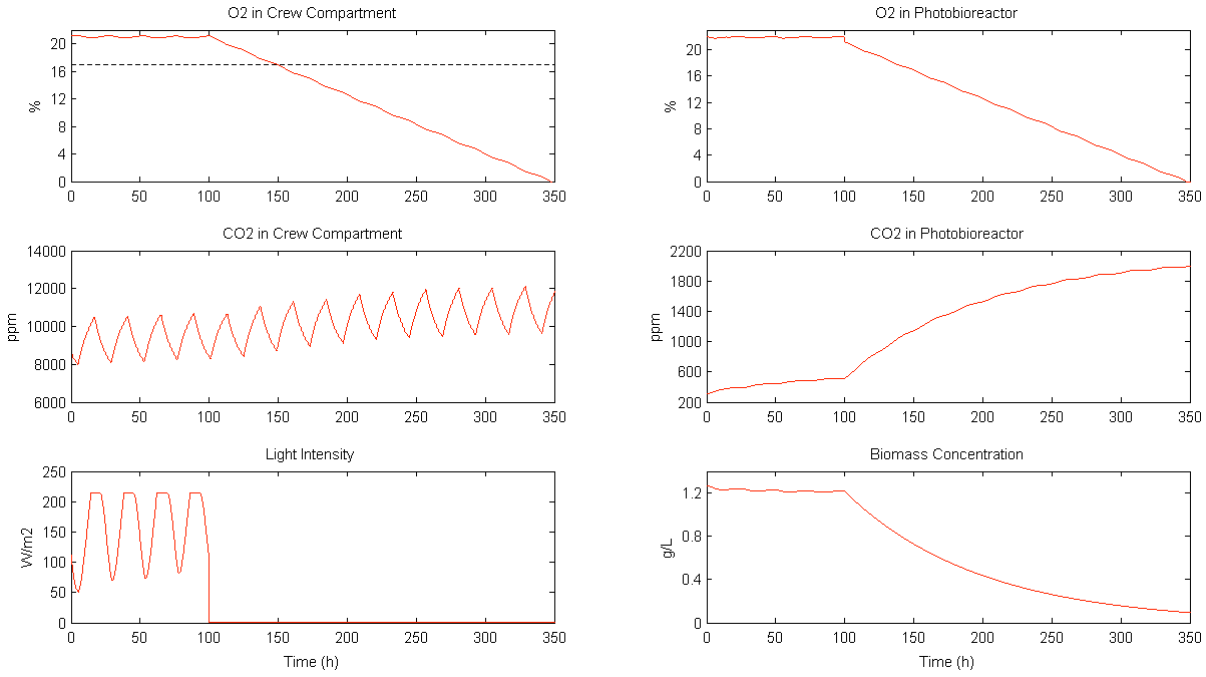

Figure 4.20 Main results for WP1 test with a sudden stop of the illumination system

- Maximum illumination

Following the case analysed before, another perturbation interesting to simulate would be the opposite: a constant operation at full light intensity. In this case, system

would outperform its regular operation and consequences could also become negative or even catastrophic.

From **Figure 4.21**, results show how would the system behave if it were working constantly at its maximum illumination capacity. At time t=100 h, light intensity is maintained indefinitely at its maximum level. Consequently, O_2 production in photobioreactor increases as well as the biomass concentration, which stabilizes at around 1.35 g·L^{-1}. In the crew compartment, O_2 starts to accumulate progressively.

Critical point for this scenario is set at an O_2 level of 25% (see section 2.1.1). With this consideration, the reaction time in this case would be of the order of 360 hours or 15 days.

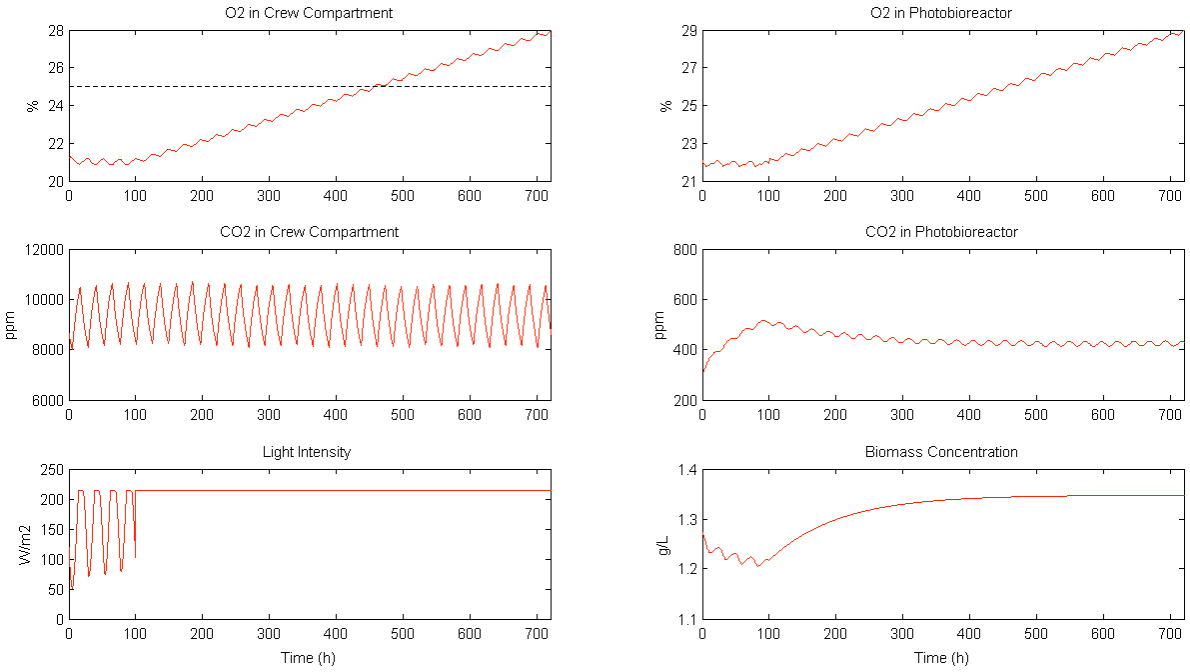

Figure 4.21 Main results for WP1 test with a continuous operation with maximum illumination

- Change in $k_L a$

$k_L a$ is the mass transfer coefficient, an important parameter within the gas/liquid mass transfer in the system described in section 2.3.5 and set to 10.5 h^{-1}. It is a parameter measured empirically and for that reason hard to predict sometimes. The consequences if $k_L a$ were assumed to be $\pm$50% of its nominal value are discussed in this section.

Figure 4.22 shows data obtained when the model is run with $k_L a$ = 5.25 h^{-1} (-50%), whereas **Figure 4.23** refers to $k_L a$ = 15.75 h^{-1} (+50%).

As can be noticed from both sets of data, differences between the two assumptions are almost negligible and results are practically the same than those obtained from the WP1 simulation in nominal conditions with $k_L a$ = 10.5 h^{-1}.

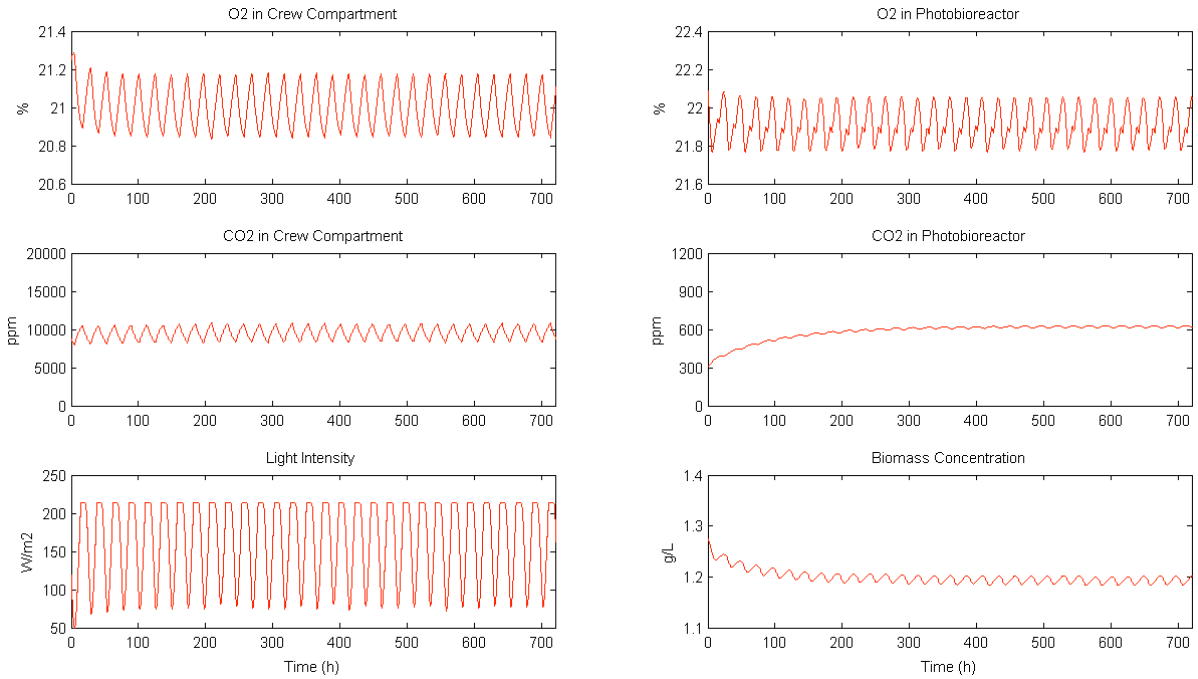

Figure 4.22 Main results for WP1 test with $k_L a$ = 5.25 h^{-1}

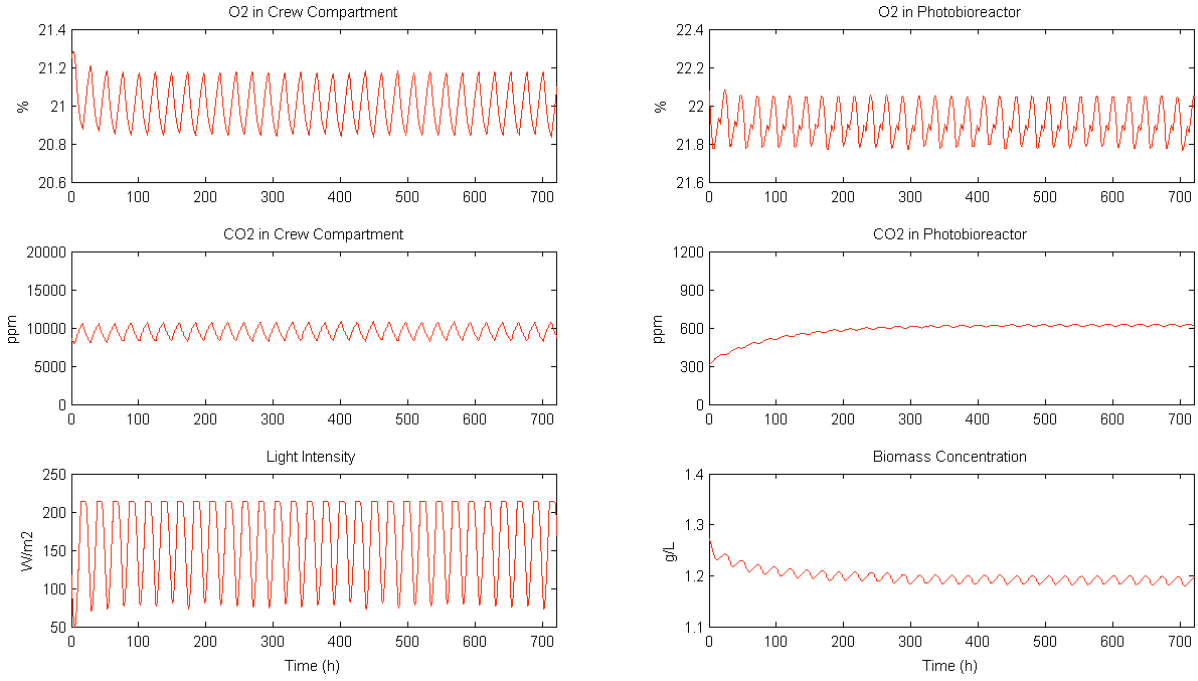

Figure 4.23 Main results for WP1 test with with $k_L a$ = 10.75 h^{-1}

- Change *Arthrospira* stoichiometry

Current stoichiometric model for *Arthrospira platensis*, defined by equation (2.8) establishes a fixed PQ of 1.444, which means that for each mole of CO_2 consumed, the culture generates 1.444 moles of O_2 by means of the photosynthesis.

The aim of this final perturbation is to see what would happen if PQ were found to be at a lower value, implying “less efficiency” in terms of O_2 production.

With PQ=1.2, the new chemical reaction could be defined by:

$$CO_2 + 0.673\,H_2O + 0.192\,HNO_3 + 0.005\,H_2SO_4 + 0.006\,H_3PO_4 \xrightarrow{light} 1.2\,O_2 + CH_{1.566}O_{0.893}N_{0.192}S_{0.005}P_{0.006} \quad \textbf{(4.1)}$$

And results obtained when running this new stoichiometric model are displayed in **Figure 4.24**, showing a quite dramatic scenario.

Due to the lower PQ, *Arthrospira platensis* produces less O_2 with the same amount of CO_2 if compared with the original model. As a result, light has to be fixed at the maximum capacity trying to compensate for the less efficient O_2 production process in the photobioreactor. Despite everything, even with the maximum light intensity, the culture is not able to satisfy the crew and O_2 level in CV gradually decreases, reaching the critical point (17%) at t=150 h. CO_2 becomes stable at levels around 9000-11000 ppm in CV and 900 ppm in CIVa. Finally, biomass concentration stabilizes at 1.35 g·L^{-1}.

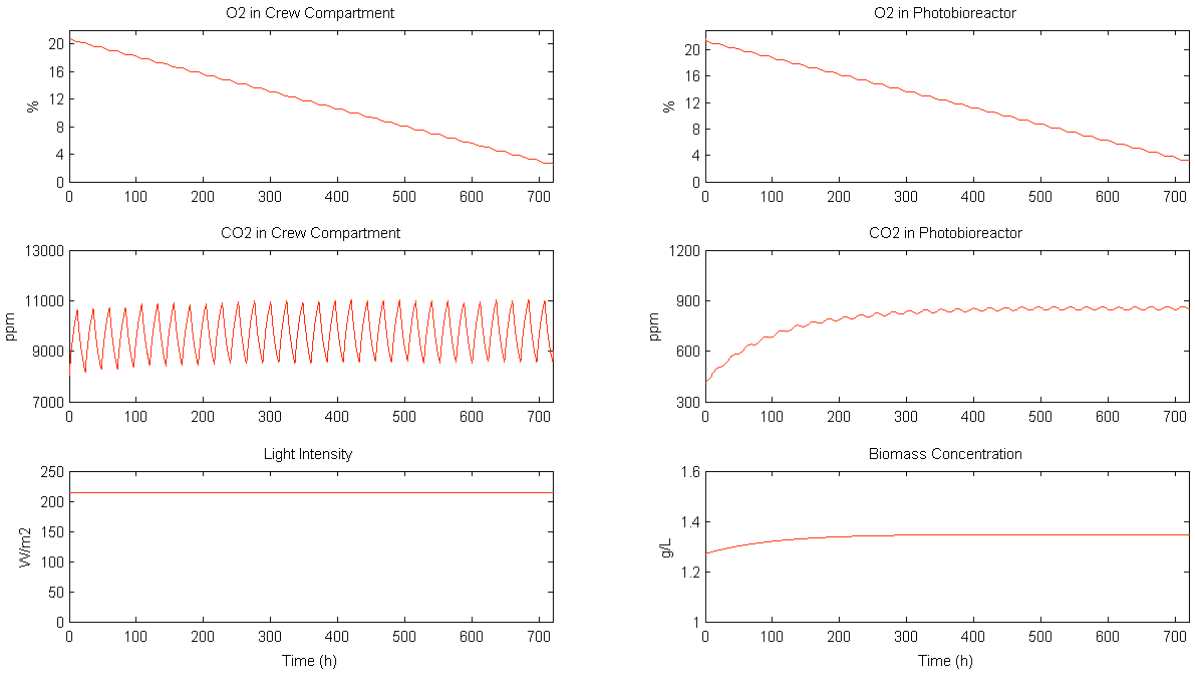

Figure 4.24 Main results for WP1 test with PQ = 1.2

Chapter 5

CONCLUSIONS

Throughout the development of the present master thesis, the main goal was to provide a simulation model to assess the current WP1 integration and to serve as a basis for a more complete model including future integration steps within the MELiSSA loop.

Based on an already existing model designed in MATLAB/SIMULINK, it was adapted to the specific operational conditions of the WP1. In addition, from the point of view of the user, the interface was slightly improved to provide a better model exploitation and understanding.

Current model was then compared with experimental data from the first WP1 integration step (21% O_2 in crew compartment) to test its validity and accuracy and two main conclusions can be extracted:

- Despite the complexity of the WP1 real system, results obtained showed in general remarkable similarities between the model and the experiment, as it is in the case of the O_2/light coupling system and the biomass concentration.

- Some evidences specially regarding the CO_2 behaviour in the system showed that some parts of the model could and should be reviewed to achieve a more realistic model.

Nevertheless, as a first point of contact between experimental and simulated data in the MELiSSA loop, the model used can be considered a great breakthrough and has numerous potential benefits.

During the development of this thesis, it has only been possible to coincide with the first WP1 integration phase, which ended by the end of June. Even so, the model has been used to simulate the remaining integration phases (18% and 23% O_2 in CV respectively), obtaining satisfactory results.

The model, in addition to be used as a support tool for WP1 integration in nominal conditions, it also allows testing different scenarios without the necessity of experiments. This feature offers a great range of possibilities before, during and after experiments are done. And this was also done in the last sections of this thesis. Perturbations were added to the system and the model was run to see the consequences in the short and long term. Results obtained are helpful to foresee, for instance, the limitations and capacities of the system.

This model can be considered as a first step towards a full MELiSSA model, containing all compartments and their interactions in a single MATLAB/SIMULINK model. Current model relies only on CV (crew compartment) and CIVa

(photobioreactor compartment), which is only a fraction of the full MELiSSA loop. However, the modularity that offers this software facilitates the process of completing the model. Thinking in the coming MELiSSA integration steps, CIII (nitrifying compartment), which is devoted to the degradation of ammonium into nitrate, would need to be included in the model, by creating its own block (and function associated) and setting the interactions between CIII, CIVa and CV.

BIBLIOGRAPHY

Public References

[1] Lasseur, C., Brunet, J., de Weever, H., Dixon, M., Dussap, C.G., Gòdia, F., Leys, N., Mergeay, M. and Van Der Straeten, D., European Space Agency, "MELiSSA: The European Project Of Closed Life Support System", *Gravitational and Space Biology,* 23(2) (2010).

[2] Gòdia, F., Albiol, J., Pérez, J., Creus, N., Cabello, F., Montràs, A., Masot, A. and Lasseur, C., "The MELISSA pilot plant facility as an integration test-bed for advanced life support systems", *Advances in Space Research,* 1483-1493 (2004).

[4] European Space Research and Technology Centre, Thermal Control and Life Support Division, "Atmosphere Quality Standards in Manned Space Vehicles", ESA-PSS-03-401 (1992).

[9] Jassby, A., "*Spirulina*: A model for microalgae as human food", Cap. 13 in *Algae and human affairs*, Ed. by Lembi, C.A. and Waaland, J.R., Cambrigde University Press, Cambridge, UK (1988).

[10] Vonshak, A. and Richmond, A., "Mass production of the blue-green alga *Spirulina*: An overview", Biomass, 15(4), 233-247 (1988).

[11] Ciferri, O. and Tiboni, O., "The Biochemistry and Industrial Potential of *Spirulina*", *Annual Review of Microbiology*, 39, 503-526 (1985).

[12] Zarrouk, C., "Contribution à l'étude d'une cyanophycée. Influence de divers facteurs physiques et chimiques sur la croissance et la photosynthèse de *Spirulina maxima* Geitler", Thèse de Doctorat, University of Paris (1966).

[13] Cogne, G., Lehmann, B., Dussap, C.G. and Gros, J.B., "Uptake of macrominerals and trace elements by the cyanobacterium *Spirulina platensis* (*Arthrospira platensis* PCC 8005) under photoautotrophic conditions: Culture medium optimization", *Biotechnology and Bioengineering,* 81(5), 588-593 (2003).

[15] He, L., Subramanian, V.R. and Tang, Y., "Experimental analysis and model-based optimization of microalgae growth in photo-bioreactors using flue gas", *Biomass and Bioenergy*, 41, 131-138 (2012).

[16] Pegallapati, A.K. and Nirmalakhandan, N., "Modeling algal growth in bubble columns under sparging with CO2-enriched air", *Bioresource Technology*, 124, 137-145 (2012).

[17] Cornet, J.F., Dussap, C.G. and Dubertret, G., "A structured model for simulation of cultures of the cyanobacterium *Spirulina platensis* in photobioreactors: I. Coupling between light transfer and growth kinetics", *Biotechnology and Bioengineering,* 40, 817-825 (1992).

[18] Cornet, J.F., Dussap, C.G., Gros, J.B., Binois, C. and Lasseur, C., “A simplified monodimensional approach for modelling coupling between radiant light transfer and growth kinetics in photobioreactors”, *Chemical Engineering Science,* 50(9), 1489-1500 (1995).

[19] Vernerey, A., “Conception, Contrôle et Fonctionnement d’un Photobioréacteur pour la culture en mode continu de la cyanobacteria *Spirulina platensis*”, Tesi Doctoral, Universitat Autònoma de Barcelona i Université de Technologie Compiègne (2000).

[23] Cornet, J.F. and Dussap, C. G., “A Simple and Reliable Formula for Assessment of Maximum Volumetric Productivities in Photobioreactors”, *Biotechnology Progress,* 25, 424-435 (2009).

Internal and Confidential Documents

[3] Peiro, E., Fossen, A., Gòdia, F. and Lamaze, B., “MELiSSA Pilot Plant: Specifications for Work Package nº1 Consultancy Study”, Memorandum of Understanding ESTEC 4000 100 293/10/NL/PA (2013).

[5] Peiro, E., Iribarren, B., Gòdia, F. and Lamaze, B., “MELiSSA Pilot Plant Frame Contract 2013-2016: WP1 Test Plan”, Memorandum of Understanding ESTEC 4000 100 293/10/NL/PA (2015).

[6] Compartment V Design Report

[7] Compartment IVa Design Report

[8] Vergara, P. and Vidal, S., “Animal Model for MELiSSA Pilot Plant”, MPP-TN-08-5001.

[14] Cornet, J.F., Dussap, C.G. and Gros, J.B., "Modelling of physical limitations in photobioreactors. Application to simulation and control of the *Spirulina* compartment of the MELiSSA artificial ecosystem”, MELiSSA Technical Note 19.2, MELISSA. Contract PRF 13O820 (1993).

[20] Mansur, M., Moyano, R., Peiro, E., Fossen, A. and Gòdia, F., “MELiSSA Pilot Plant: Test report for gas-liquid mass transfer analysis of C4a bioreactor”, MELiSSA Technical Note 87.2.13 Part 2 Section 3, Memorandum of Understanding ESTEC 4000 100 293/10/NL/PA (2012).

[21] Poughon, L., "MELiSSA simulation and modelling: Gas streams", MELiSSA Technical Note 17.1, ESTEC CONTRACT 8125/88/NL/FG - CCN4 (1994).

[22] Poughon, L., "Dynamic modelling of a coupled MELiSSA crew – compartment C4a with Matlab/Simulink", MELiSSA Technical Note 83.2, ESA/ESTEC CONTRACT Memorandum of Understanding 1907105/NL/CP (2007).